

Sensitive compounds as ACI-RCC cell inhibitors

Category	Compound	% DMSO
Antitumor (estrogen receptor)	Tamoxifen, citrate	5.2
Antitumor (DNA)	Daunorubicin, HCl	7.4
Antitumor (DNA)	Doxorubicin, HCl	9.2
Heat shock protein 90	Radicalol	3.5
Heat shock protein 90	17-Allylamino-17-demethoxygeldanamycin (tanespimycin)	14.6
Protein kinase C	Bisindolymaleimide I, HCl	9.7
Protein kinase C	Go7874	0.5
Protein kinase C, A, G, myosin light chain kinase	Staurosporine	2.1
V-adenosine triphosphatase	Bafilomycin A1	8.2
Cathepsin G	Z-gly-leu-phe-chloromethyl ketone	5.2
Na ionophore	Monensin	7.8
K ionophore	Nigericin	3.4
Guanylate cyclase	LY 83583	0.8
Hypoxia-inducible factor	Chetomin	1.4
Spermidine/spermine N1-acetyltransferase activator	N1, N12-dioethylspermine (BESpm)	0.5
Akt	Akt inhibitor IV	0.4
Bruton's tyrosine kinase	Terric acid	9.7
Hepatocyte growth factor receptor/Met	SU11274	8.7
Platelet-derived growth factor	SU11652	0.2

Luc can catabolize a substrate D-luciferin, which is relatively stable *in vivo*. Using the newly established bioluminescent rat RCC cell line we developed a novel system to test *in vitro* and *in vivo* tumor growth.

We first examined the *in vitro* characteristics of 2 Luc labeled ACI-RCC cell lines. ACI-RCC-cbLuc cells were superior to ACI-RCC-ffLuc cells for *in vitro* measurement in terms of luminescence intensity with a much lower detection limit. As reported in previous studies of other tumor models, the number of tumor cells *in vitro* correlated with the bioluminescence signal, indicating the quantitative value of this system for *in vitro* measurement (fig. 2). This appeared reproducible in solid tumors but not in an IL-3 dependent murine leukemia cell line, in which signal intensity was affected by IL-3 concentration and proliferation stage.¹²⁻¹⁴

We then examined *in vivo* the growth of these luciferase labeled ACI-RCC cell lines. ACI-RCC-cbLuc cells were rejected completely by syngeneic ACI rats while ACI-RCC-ffLuc cells were consistently taken to establish tumors. This difference may be due to the higher antigenicity of Luc protein derived from *Phototinus plagiophthalmus*, which predisposes ACI-RCC-cbLuc cells to increased susceptibility to attack by the host cellular immune defense system. This susceptibility may be explained by the fact that ACI-RCC-cbLuc cells grew in athymic mice. Even with syngeneic transplantation transplanted cells expressing a marker protein such as green fluorescent protein and β -galactosidase (LacZ) occasionally disappear due to immunogenicity.^{15,16} Even ffLuc, which is considered less immunogenic than green fluorescent protein,¹⁷ has been reported to induce a T-helper type 1 immune response after intradermal immunization in immune competent Balb/c mice.¹⁸

These factors may subsequently raise the question of the difference in antigenicity between ACI-RCC-ffLuc and ACI-RCC-cbLuc cells. The quantity or quality of Luc protein expressed in each cell line must be considered, although it is hard to accurately compare the differences. We assume that the former is less likely to be the reason for the different fates *in vivo* of the 2 cell lines. This assumption is supported by the finding that enhanced ffLuc expression in mouse T cells permitted sensitive tracking of adoptively transferred T cells infiltrating tumor sites without increasing immunogenicity in immunocompetent murine models.¹⁹ Thus, immune responses involving the different Luc proteins may have to be considered cautiously. Thereafter we focused on ACI-RCC-ffLuc cells to investigate *in vivo* tumor growth using an *in vivo* imaging system.

A significant correlation between luminescence intensity and subcutaneous tumor volume verified the quantifiable nature of our Luc labeled tumor model system (fig. 5, B). Because of the impossibility of measuring tumor size using calipers in orthotopic RCC models, therapeutic experiments are usually assessed by animal symptoms and end point variables, such as survival time, kidney weight and histological analysis of explanted kidneys. However, our system enabled noninvasive real-time extracorporeal monitoring of orthotopic tumors beneath the renal capsule. Notably subsequent metastasis of the orthotopic tumor to the lung could also be monitored (fig. 6, B). This metastatic pattern, similar to the RENCA model, mimics that in human RCC, which is clinically meaningful for studying RCC progression.

Our use of rats rather than mice was also advantageous for BLI. Easy intravenous delivery of the substrate D-luciferin enabled rapid, stable measure-

ment of bioluminescence intensity. Photon counts measured by IVIS peaks 1 minute after intravenous injection of D-luciferin had fewer individual differences in our models (data not shown). The window of reliable maximum photon emission in murine models requiring intraperitoneal injection of Luc varies among studies and is reportedly much longer, usually 15 minutes or more.^{12,20,21}

Finally, we examined the use of our Luc labeled rat RCC cell line ACI-RCC-cbLuc as an *in vitro* screening tool for anticancer agents. The results of drug sensitivity using the SCADS inhibitor kit combined with Luc labeled cells provided a useful screening tool with rapid high throughput. Screened compounds with an inhibitory effect on ACI-RCC cells included molecules related to RCC progression, ie heat shock protein 90, AKT, Met and platelet-derived growth factor, which are molecular targets of recent RCC therapies (see table).^{3,22,23} These results imply the practical accuracy and feasibility of our systems for *in vitro* RCC investigation. The exact efficacy and toxicity of such screened compounds *in vivo* as well as appropriate combinations are under investigation at our laboratory.

CONCLUSIONS

We engineered Luc expressing cancer cells from a newly established rat RCC cell line arising from immunocompetent rats, and noted easy quantitative detection of orthotopic tumor growth and metastatic spread in real time using the Luc based bioluminescent systems. We also introduced a feasible method of *in vitro* screening for anticancer compounds using Luc labeled rat RCC cells. This Luc based *in vivo* model system coupled with the *in vitro* screening system may facilitate the development of new therapies that may eradicate metastatic RCC. Also, our allograft tumor model in an immunocompetent animal may be advantageous for studying exact treatment efficacy and safety for immunogenic tumors such as RCC.

ACKNOWLEDGMENTS

The Screening Committee of Anticancer Drugs provided the SCADS inhibitor kit.

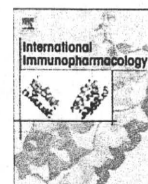
REFERENCES

- Mulders P, Figlin R, deKernion JB et al: Renal cell carcinoma: recent progress and future directions. *Cancer Res* 1997; **57**: 5189.
- Hutson TE and Quinn DI: Cytokine therapy: a standard of care for metastatic renal cell carcinoma? *Clin Genitourin Cancer* 2005; **4**: 181.
- Rini BI: Vascular endothelial growth factor-targeted therapy in renal cell carcinoma: current status and future directions. *Clin Cancer Res* 2007; **13**: 1098.
- Lyons SK: Advances in imaging mouse tumour models *in vivo*. *J Pathol* 2005; **205**: 194.
- Wiltrout RH, Gregorio TA, Fenton RG et al: Cellular and molecular studies in the treatment of murine renal cancer. *Semin Oncol* 1995; **22**: 9.
- Nogawa M, Yuasa T, Kimura S et al: Monitoring luciferase-labeled cancer cell growth and metastasis in different *in vivo* models. *Cancer Lett* 2005; **217**: 243.
- Verheul HM, Hammers H, van Erp K et al: Vascular endothelial growth factor trap blocks tumor growth, metastasis formation, and vascular leakage in an orthotopic murine renal cell cancer model. *Clin Cancer Res* 2007; **13**: 4201.
- Kato Y, Yoshimura K, Shin T et al: Synergistic *in vivo* antitumor effect of the histone deacetylase inhibitor MS-275 in combination with interleukin 2 in a murine model of renal cell carcinoma. *Clin Cancer Res* 2007; **13**: 4538.
- Okada S, Hamazaki S, Ebina Y et al: Nephrotoxicity and induction of the renal adenocarcinoma by ferric-nitritotriacetate (Fe-NTA) in rats. In: *Structure and Function of Iron Storage and Transport Proteins*. Edited by I Urushizaki. Amsterdam: Elsevier Science 1983; pp 473-478.
- Kobayashi M, Okada T, Murakami T et al: Tissue-targeted *in vivo* gene transfer coupled with histone deacetylase inhibitor depsipeptide (FK228) enhances adenoviral infection in rat renal cancer allograft model systems. *Urology* 2007; **70**: 1230.
- Lu X, Kallinteris NL, Li J et al: Tumor immunotherapy by converting tumor cells to MHC class II-positive, Ii protein-negative phenotype. *Cancer Immunol Immunother* 2003; **52**: 592.
- Jenkins DE, Oei Y, Hornig YS et al: Bioluminescent imaging (BLI) to improve and refine traditional murine models of tumor growth and metastasis. *Clin Exp Metastasis* 2003; **20**: 733.
- Rehemtulla A, Stegman LD, Cardozo SJ et al: Rapid and quantitative assessment of cancer treatment response using *in vivo* bioluminescence imaging. *Neoplasia* 2000; **2**: 491.
- Inoue Y, Tojo A, Sekine R et al: *In vitro* validation of bioluminescent monitoring of disease progression and therapeutic response in leukaemia model animals. *Eur J Nucl Med Mol Imaging* 2006; **33**: 557.
- Brubaker JO, Thompson CM, Morrison LA et al: Th1-associated immune responses to beta-galactosidase expressed by a replication-defective herpes simplex virus. *J Immunol* 1996; **157**: 1598.
- Gambotto A, Dworacki G, Cicinnati V et al: Immunogenicity of enhanced green fluorescent protein (EGFP) in BALB/c mice: identification of an H2-Kd-restricted CTL epitope. *Gene Ther* 2000; **7**: 2036.
- Hakamata Y, Murakami T and Kobayashi E: "Firefly rats" as an organ/cellular source for long-term *in vivo* bioluminescent imaging. *Transplantation* 2006; **81**: 1179.
- Jeon YH, Choi Y, Kang JH et al: Immune response to firefly luciferase as a naked DNA. *Cancer Biol Ther* 2007; **6**: 781.
- Rabinovich BA, Ye Y, Etto T et al: Visualizing fewer than 10 mouse T cells with an enhanced firefly luciferase in immunocompetent mouse models of cancer. *Proc Natl Acad Sci U S A* 2008; **105**: 14342.
- Peter C, Kielstein JT, Clarke-Katzenberg R et al: A novel bioluminescent tumor model of human renal cancer cell lines: an *in vitro* and *in vivo* characterization. *J Urol* 2007; **177**: 2342.
- Smakman N, Martens A, Kranenburg O et al: Validation of bioluminescence imaging of colorectal liver metastases in the mouse. *J Surg Res* 2004; **122**: 225.
- Ronnen EA, Kondagunta GV, Ishill N et al: A phase II trial of 17-(Allylamino)-17-demethoxygeldanamycin in patients with papillary and clear cell renal cell carcinoma. *Invest New Drugs* 2006; **24**: 543.
- Bellon SF, Kaplan-Lefko P, Yang Y et al: c-Met inhibitors with novel binding mode show activity against several hereditary papillary renal cell carcinoma-related mutations. *J Biol Chem* 2008; **283**: 2675.



Contents lists available at ScienceDirect

International Immunopharmacology

journal homepage: www.elsevier.com/locate/intimp

Preliminary report

Chemopreventive anti-cancer agent acyclic retinoid suppresses allogeneic immune responses in rats

Ichiro Ohsawa^{a,b}, Takashi Murakami^{a,c,*}, Lei Guo^d, Shin Enosawa^d, Naoto Ishibashi^e, Shuji Isaji^b, Shinji Uemoto^f, Eiji Kobayashi^a^a Division of Organ Replacement Research, Center for Molecular Medicine, Jichi Medical University, 3311-1 Yakushiji, Shimotsuke, Tochigi 329-0498, Japan^b Department of Hepatobiliary Pancreatic and Transplant Surgery, Mie University, 2-174 Edobashi, Tsu, Mie 514-8507, Japan^c Division of Bioimaging Sciences, Center for Molecular Medicine, Jichi Medical University, 3311-1 Yakushiji, Shimotsuke, Tochigi 329-0498, Japan^d Department of Innovative Surgery, National Research Institute for Child Health and Development, 2-10-1 Okura, Setagaya, Tokyo 154-8567, Japan^e Tokyo New Drug Research Laboratories, Kowa Co., Ltd., 2-17-43 Noguchi, Higashimurayama, Tokyo 189-0022, Japan^f Department of Hepatobiliary Pancreatic Surgery and Transplantation, Kyoto University, 54 Shogoin-Kawaramachi, Sakyo, Kyoto 606-8507, Japan

ARTICLE INFO

Article history:

Received 3 December 2009

Received in revised form 15 April 2010

Accepted 22 April 2010

Keywords:

Acyclic retinoid

Anti-cancer drug

Chemoprevention

Immunosuppression

Rat

ABSTRACT

Acyclic retinoid NIK-333 (ACR) is a chemopreventive agent that acts by suppressing the recurrence of hepatocellular carcinoma (HCC) following initial treatment and is now being employed in clinical trials. The chemopreventive effects of ACR have been analyzed from various aspects, and it is well known that some retinoic acid (RA) derivatives affect host immunity. The objective of this study is to investigate the effects of ACR on host immunity. The results demonstrated that ACR prolonged heart and liver graft and recipient survival in rat allogeneic organ transplantation. The immunosuppressive effect of ACR administered at 100 mg/kg/day was almost equivalent to that of CsA administered at 1 mg/kg/day *in vivo*. In the mixed lymphocyte reaction (MLR), ACR suppressed lymphocyte proliferation non-specifically. Gene expression analysis of splenic lymphocytes from ACR-treated recipient rats revealed no distinct change in Interleukin (IL)-2 and increases in Interferon (IFN)-gamma. In conclusion, ACR possesses immunosuppressive potential *in vivo* and is a promising chemopreventive drug for long term use against HCC.

Crown Copyright © 2010 Published by Elsevier B.V. All rights reserved.

1. Introduction

It has been argued since the latter 1960s that retinoic acid (RA) and derivatives may have an effect on the immune system [1]. Most of these reports referred to the enhancement of host immunocompetency following the administration of RA [2–4]. However, it has recently become clear that some RA derivatives possess immunosuppressive or graft protection effects [5–8]. These findings suggest that each RA derivative possesses a unique character in terms of its effect on immuno-regulatory functions.

Abbreviations: ACR, acyclic retinoid; ConA, Concanavalin A; CsA, cyclosporin A; FCS, fetal calf serum; GAPDH, glyceraldehyde-3-phosphate dehydrogenase; HCC, hepatocellular carcinoma; HHT, heterotopic heart transplantation; MLR, mixed lymphocyte reaction; IFN, interferon; IL, interleukin; OLT, orthotopic liver transplantation; RA, retinoic acids; RAR, retinoic acid receptor; RXR, retinoid-X receptor; SI, stimulation index; ATRA, tretinoin.

* Corresponding author. Division of Bioimaging Sciences, Center for Molecular Medicine, Jichi Medical University, 3311-1 Yakushiji, Shimotsuke, Tochigi 329-0498, Japan. Tel.: +81 285 58 7446; fax: +81 285 44 5365.

E-mail addresses: ohsawa-i@clin.medic.mie-u.ac.jp (I. Ohsawa), takmu@jichi.ac.jp (T. Murakami), leiguo12@hotmail.com (L. Guo), senosawa@nch.go.jp (S. Enosawa), n-isibas@kowa.co.jp (N. Ishibashi), isaji-s@clin.medic.mie-u.ac.jp (S. Isaji), uemoto@kuhp.kyoto-u.ac.jp (S. Uemoto), eijikoba@jichi.ac.jp (E. Kobayashi).

Acyclic retinoid NIK-333 (ACR), an analogue of RA, has been shown to suppress secondary hepatocellular carcinoma (HCC) following initial resection or ablation [9]. These chemopreventive effects of ACR have been analyzed from various aspects [10–15]. While many RA analogues have been considered as promising anti-cancer agents [16], they might also modulate host immune reactions [17]. In this study, we examined the effects of ACR on the host and cancer using an allogeneic cardiac transplantation model and a syngeneic tumor-implanted model in rats, respectively.

2. Materials and methods

2.1. Animals and cells

Inbred male DA (RT1^a), LEW/DuCrj (RT1^b) and F344/DuCrj (RT1^{lv}) rats were purchased from Charles River Japan Inc. (Yokohama, Japan), and BN (RT1ⁿ) and PVG (RT1^c) rats were purchased from SLC Inc. (Hamamatsu, Japan). Rats were used at 8–10 weeks of age, and all experiments in this study were performed in accordance with the Guidelines for the Care and Use of Laboratory Animals of the Jichi Medical University and National Research Institute for Child Health and Development. The RCN-H4 cell line has been established as a highly liver-metastatic subline of the RCN9 parental cell line derived from

F344/DuCrj rat (Riken Cell Bank, Tsukuba, Japan) [18]. Luciferase-transduced luc-RCN-H4 cells [19] were maintained in RPMI 1640 medium (Sigma-Aldrich, Taufkirchen, Germany) supplemented with 10% fetal calf serum (FCS) (ICN-Flow, Aurora, OH) and penicillin-streptomycin (Gibco BRL, Grand Island, NY) at 37 °C in a humidified atmosphere of 5% CO₂.

In vivo implantation of luc-RCN-H4 cells and tumor progression monitoring using the noninvasive IVIS bio-imaging system (Xenogen, Alameda, CA) were as previously described [19]. Heterotopic heart transplantation (HHT) and orthotopic liver transplantation (OLT) were performed using a modified method of Olausson [20] and Kamada [21]. For the HHT, the graft beating was examined daily by palpitation, and functional graft rejection was defined as the day when the heart grafts ceased beating.

2.2. Reagents

ACR [(2E,4E,6E,10E)-3,7,11,15-tetramethyl-2,4,6,10,14-hexadecapentaenoic acid, C₂₀H₃₀O₂] (official name; NIK-333) was synthesized and kindly provided by Kowa Co., Ltd. (Tokyo, Japan). Cyclosporin A (CsA) was purchased from Wako Pure Chemical Industries, Ltd. (Osaka, Japan). ACR was dissolved in soybean oil and administered at 0.5 ml/100 g body weight for p.o. administration, and CsA was dissolved in olive oil and used at 0.15 ml/100 g body weight for p.o. administration or suspended in saline at a concentration of 1 mg/ml for s.c. injection. A stomach tube was used for the p.o. administration.

2.3. Mixed lymphocyte reaction (MLR)

Splenic lymphocytes were prepared by passing minced tissue through a cell strainer followed by density gradient centrifugation using Lympholyte-Rat (Ontario, Canada). Irradiated stimulator cells (1 × 10⁵) were cultured for 72 h with responder cells (1 × 10⁵) in 200 μl RPMI1640 medium supplemented with 10% FCS on a 96-well plate at 37 °C in a humidified atmosphere of 5% CO₂. Lymphocytes from BN rat were used as third-party, and Concanavalin A (ConA) was used as the control stimulant. Twenty-four hours prior to termination of the culture, 1 μCi of [³H]-thymidine (Amersham Pharmacia Biotech, Amersham, UK) was added to each well. [³H]-thymidine uptake was determined using a liquid scintillation counter (Packard Japan, Tokyo, Japan). Each [³H]-thymidine uptake count (count per minute; cpm) was expressed in the form of a stimulation index (SI), which was calculated as follows:

$$\text{Stimulation Index} = \frac{\text{Experimental group (cpm)}}{\text{Syngeneic control (cpm)}}$$

Table 1
Graft/recipient survival under ACR or CsA administration in rat heterotopic heart/orthotopic liver transplantation.

Graft	Combination	Drug	Dose (mg/kg/day)	N	Graft/recipient survival (days) (Ave.)	p value
Heart	PVG–PVG	Vehicle	–	8	>15(8)	>15.0
		Vehicle	–	9	6, 6, 6, 7, 7, 7, 8, 8	6.9
	DA–PVG	ACR	10	5	7, 7, 8, 8, 8	7.6
		ACR	25	5	7, 8, 8, 8, 9	8.0
		ACR	100	6	8, 9, 10, 10, 10, 13	10.0
		CsA	1	5	8, 8, 8, 12, 13	9.8
		CsA	10	4	>15, >15, >15, >15	>15.0
		CsA	100	5	4, 4, 5, 5a, 6a	4.8
	DA–LEW	Vehicle	–	5	5, 7a, 7a, 9	7.0
	Liver	LEW–LEW	Vehicle	–	4	>60, >60, >60, >60
Vehicle			–	6	10, 11, 11, 11, 12, 12	11.2
DA–LEW		ACR	10	3	18, 21, 51	30.0
		ACR	25	5	14, 18, 20, 25, 38	23.0
		ACR	50	2	26, 27	26.5
		ACR	100	2	17, 19	18.0

ACR; p.o., CsA; i.m., a; splenectomy for MLR at day 7.

2.4. Reverse-transcriptase polymerase chain reaction

Total RNA was extracted from spleen cells using Isogen (Nippon Gene, Toyama, Japan) as previously described [19]. The following primers were used: glyceraldehyde-3-phosphate dehydrogenase (GAPDH) sense, 5'-GTA TCG TGG AAG GAC TCA TG-3'; GAPDH anti-sense, 5'-AGT GGG TGT CGC TGT TGA AG-3'; IFN-γ sense, 5'-CCC TCT CTG GCT GTT ACT GC-3'; IFN-γ anti-sense, 5'-CTC CTT TTC CGC TTC CTT AG-3'; IL-2 sense, 5'-GCG CAC CCA CTT CAA GCC CT-3'; and IL-2 anti-sense, 5'-CCA CCA CAG TTG CTG GCT CA-3. The PCR conditions for each set of primers comprised heating at 94 °C for 2 min, followed by 35 cycles at 94 °C for 15 s, 57 °C for 30 s and 68 °C for 2 min. The PCR products were analyzed electrophoretically using a 1% agarose gel.

2.5. Cell proliferation assay

luc-RCN-H4 cells (4.0 × 10⁴) were plated in triplicate onto 48-well plates and incubated in the presence of ACR at the indicated concentrations. Following 48 h incubation, luc-RCN-H4 cells were collected from each well and then counted using a hemacytometer.

2.6. Statistical analysis

Results are expressed as mean ± standard deviation (SD) and analyzed using a one-way analysis of variance (ANOVA) or unpaired Student's *t*-test for statistical evaluation. Graft and recipient survival data derived from the cardiac and liver transplantation experiments were analyzed using a Log-rank test. Differences among groups were considered significant if the *p* value was less than 0.05. The data are expressed as the means ± SD. All analyses were performed using the StatView ver. 5.0 software program (SAS Institute, Cary, NC).

3. Results

3.1. Immunologic effects in rat organ transplantation

In an effort to investigate the effect of ACR on host immunity, we initially conducted heterotopic heart transplantation (HHT) of rats (Table 1). In a preliminary toxic study in rats, ACR administration at a dose of 100 mg/kg/day for 4 weeks resulted in neutrophilia, low albumin, high alkaline phosphatase and high total cholesterol in blood, and caused no pathological change on rat spleen. Although administration of ACR at a dose of 200 mg/kg/day for the same duration did not result in any deaths, several serious adverse effects resulted such as anemia, body weight loss or bone fracture. Based on these observations, this study employed doses of 10, 25, 50 and 100 mg/kg/day. With HHT from a

DA donor to a PVG recipient, ACR significantly prolonged cardiac graft survival at a dose of 25 mg/kg/day. This graft prolongation effect occurred in a dose-dependent manner, and ACR administration at 100 mg/kg/day showed a significant immunosuppressive effect almost equivalent to that resulting from CsA administration at 1 mg/kg/day. This immunosuppressive effect was also shown in the rat DA to LEW combination, which causes severe immunological rejection, with significant differences. We then evaluated the immunosuppressive effect of ACR in a rat orthotopic liver transplantation (OLT) model (Table 1). With OLT from a DA donor to a LEW recipient, ACR demonstrated a significant graft prolongation effect even at relatively low administration dose (10 mg/kg/day). Unlike the case with HHT, a dose-dependent effect was not observed in recipient rat survival with OLT. Interestingly, the mean survival with OLT was greatest with an administration dose of 10 mg/kg/day, although use of a liver transplantation model is not always the most appropriate method for the evaluation of immunosuppressive effects. Unlike the case with HHT, OLT in rats administered with ACR at 100 mg/kg/day resulted in short term diarrhea and more body weight loss following transplantation, with the possibility that the body weight loss influenced survival (data not shown). These results indicate that ACR can induce a graft prolongation effect on allogeneic organ transplantation, suggesting that ACR possesses immunosuppressive activity.

3.2. Effect of ACR on lymphocyte proliferation

We then set out to determine whether ACR can suppress allogeneic immune responses *in vitro*. The MLR assay was performed using lymphocytes isolated from the spleen of recipient LEW rats at 5 to 7 days post-transplantation. As shown in Fig. 1A, the stimulation index (SI) was significantly suppressed in lymphocytes isolated from ACR-administered LEW recipients (against DA donors). Furthermore, a similar suppression of MLR with ACR was observed against stimulant by third-party, indicating that ACR is able to suppress non-specific allogeneic immune responses. ACR was also able to suppress lymphocyte proliferation stimulated by ConA. These results demonstrate that ACR can non-specifically suppress lymphocyte proliferation. The observed immunosuppressive effect of ACR is not strong enough for it to be employed in the area of clinical immunosuppression.

Gene expression analysis of splenic lymphocytes from ACR-treated recipient rats revealed no distinct change in IL-2 and increases in IFN- γ (Fig. 1B). These results suggest that ACR does not affect IL-2 mRNA

expression and can suppress lymphocyte proliferation. It was noted that the augmentation in IFN- γ expression was not inhibited by ACR, suggesting that ACR does not completely suppress host immune responses.

3.3. Effect of ACR on luc-RCN-H4 colon cancer cells

In an effort to determine the effect of ACR on cancer cell growth, ACR was administered to luc-RCN-H4 colon cancer cells *in vitro* (Fig. 2A). ACR was able to inhibit cell proliferation when present at a concentration greater than 50 μ M. CsA administration showed marked inhibition at a concentration of 16 μ M, which was presumed to involve a toxic effect (Fig. 2B). To examine the anti-tumor effect of ACR *in vivo*, luc-RCN-H4 cells were injected into the ileocolic vein of F344/DuCrj rats [19] and followed by daily administration of ACR sufficient to suppress HCC development by 3'-methyl-4-dimethylaminoazobenzene (80 mg/kg/day). Tumor progression was monitored by *in vivo* luminescent imaging [19]. In comparison with the control treatment (soybean oil), ACR exerted no significant influence on tumor-derived photons in the liver, indicating that ACR had no effect on tumor growth at this dosage (Fig. 2C). This observed *in vivo* anti-tumor effect was the same when lower doses of ACR were employed (data not shown). Although increasing the dosage of ACR might have resulted in a tumor-suppressing effect in this model, the use of doses over 100 mg/kg/day resulted in some adverse effects in the preliminary toxic test. On the other hand, although the use of CsA at 3 mg/kg/day showed no promotion effect, use at 15 mg/kg/day exerted promotion effects on tumor growth (Fig. 2D). We concluded that the use of ACR at the normal dose of 100 mg/kg/day does not show tumor promotion effects against luc-RCN-H4 colon cancer progression *in vivo*.

4. Discussion

RA is often recognized as an essential substance for homeostasis [16]. RA can facilitate passage of various immature cells, including malignant cells, to terminal differentiation through receptors that are widely distributed in the body [22,23]. These RA receptors fall into two groups comprising retinoic acid receptors (RARs) and retinoid-X receptor (RXRs), with each group being further classified into subtypes comprising RAR α , β , γ and RXR α , β , γ , respectively. The distribution of these receptors on the cell surface and ligand affinities regulate the effectiveness of RA compounds, and it is thought that this determines

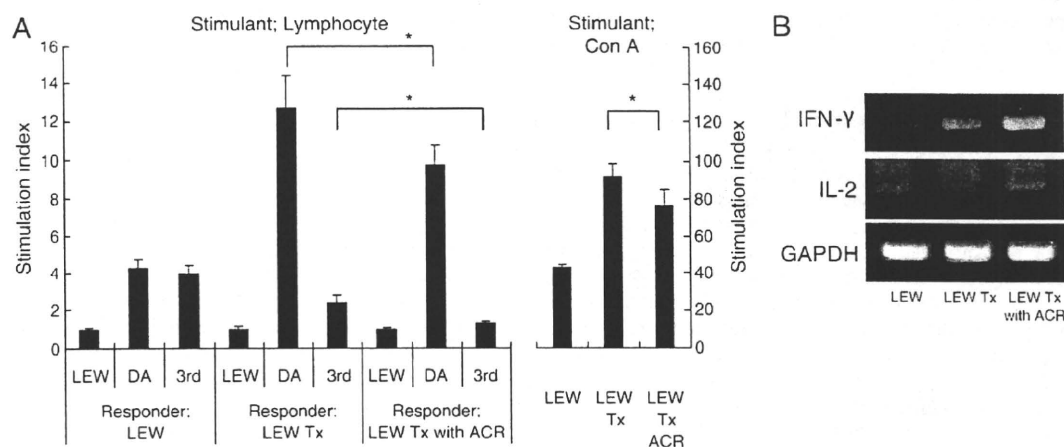


Fig. 1. ACR suppressed lymphocyte proliferation in the mixed lymphocyte reaction (MLR) (A, representative data). Responder cells were collected from removed spleen following graft rejection, as indicated in Table 1A. In experiments using naïve DA lymphocytes as stimulant, lymphocytes from graft-implanted rat showed intense proliferation compared with control LEW. This proliferation was suppressed by ACR administration. Suppression of proliferation by ACR was also observed in experiments using naïve BN lymphocytes as third-party stimulant and in experiments using Con A as stimulant. The original control cpm values were as follows; (Stimulant–Responder) LEW–LEW 3687.2, LEW–LEW Tx 1555.5, LEW–LEW Tx with ACR 1368.8. Gene expression analysis of spleen cells revealed that, unlike the case with IL-2, IFN- γ expression increased in ACR-administered recipients (B). *, $p < 0.05$.

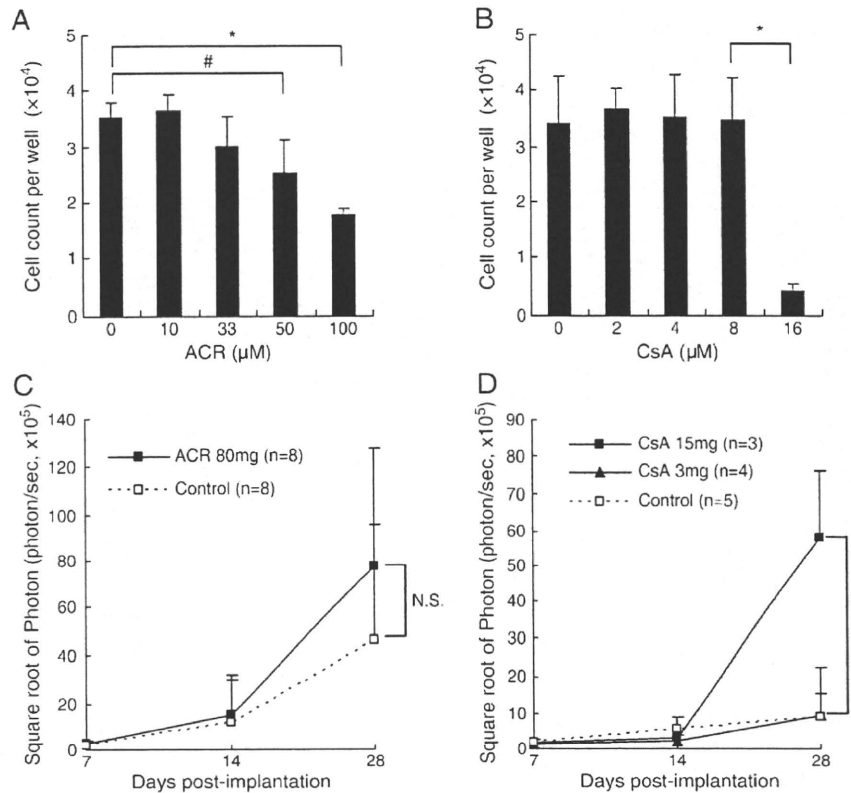


Fig. 2. Anti-tumor activity of ACR on luc-RCN-H4 cells *in vitro* and *in vivo*. In the cell growth assay, ACR showed growth inhibitory effects but only at levels above physiological concentrations (A). CsA administration showed marked inhibition at a concentration of 16 μM , which was presumed to involve a toxic effect (B). *In vivo* experiment, 5.0×10^5 luc-RCN-H4 cells in 0.5 ml PBS were injected into the ileocolic vein of rats. Luc-RCN-H4 cell-implanted rats were divided into two groups; ACR at 80 mg/kg/day and control (C), CsA at 3 mg/kg/day, 15 mg/kg/day and control (D). The metastatic fate of luciferase-positive tumor cells was followed using an *in vivo* imaging system on days 7, 14 and 28. The results showed that ACR administered at 80 mg/kg/day and CsA administered at 3 mg/kg/day had no effect on tumor growth. *, $p < 0.05$, #, $p = 0.06$.

the effects of RA at the single cell or organ levels, including cancer cells [22].

RA derivatives have been investigated as potential anti-cancer agents following the success of Tretinoin (ATRA) with promyelocytic leukemia [24]. Despite the emerging evidence, most RA derivatives do not always exert direct anti-cancer effects, and are often recognized as compounds useful in cancer chemoprevention [23]. To date, at least 7 RA analogues have been shown to possess tumor-suppressive activity clinically and experimentally [16]. ACR is one RA derivative which is presently being considered as a drug for the inhibition of HCC recurrence in clinical trials.

HHT is the most reliable model to evaluate allogeneic immune responses. Our HHT results demonstrated the substantial immunosuppressive effect of ACR (Table 1). Although the OLT results did not reveal a dose-dependent recipient survival trend, this is not surprising given that recipient survival following orthotopic liver transplantation was not always simply correlated with host immune conditions, especially in cases when the administered drug targeted the implanted graft. Our MLR experiments also demonstrated immunosuppression by ACR *in vitro*, supporting the *in vivo* immunosuppressive role of ACR in allogeneic immune responses. In this study, although no attempt was made to identify the mediator(s) or factor(s) involved in the ACR immunosuppressive effect, previous studies have reported the mechanism by which RA changes the leukocyte population and immunity of the host without IL-2 mediation [7,17]. Our results follow on from these reports in terms of outlining the immunosuppressive efficacy of RA derivatives.

Various reports have referred to the anti-tumor effect of RA derivatives in tumor implantation models [25,26]. Our *in vivo* experi-

ments showed that although ACR administered at 80 mg/kg/day did not have any influence on tumor growth, the proliferation of luc-RCN-H4 cells *in vitro* was inhibited by ACR. This result should be interpreted by considering the following: (1) although the *in vitro* anti-cancer effect of ACR has been investigated in several studies as described above [10,11,13–15], these effects could not easily be analyzed *in vivo* since ACR is not a typical anti-cancer agent but a chemopreventive compound, and (2) the chemopreventive effect of ACR *in vivo* has already been proven clinically by Muto, et al. [9] and experimentally by Kagawa, et al. [12], and both studies included observations over a long time period. Therefore, we focus on our experimental results showing that the proliferation of implanted luc-RCN-H4 cells was not promoted by ACR. We supposed that a compound with immunosuppressive potential could be categorized into one of two groups according to its influence on cancer cell proliferation, being promotion [19,27–29] or suppression [30–33]. Needless to say, it is impossible to clearly make this assignment since the criteria employed to categorize a compound differ depending on the conditions of each study or experiment, although the fact that a compound does not possess the potential to promote cancer cell proliferation is the most important in a clinical situation. In this regard, we may suggest that ACR does not possess the potential to promote cancer cell proliferation in our experiments. Although we did not test ACR at doses greater than 100 mg/kg/day, clinical studies of ACR administered at 600 mg/body/day [9] and animal experiments involving administration of ACR at 80 mg/kg/day [12] should confirm the sufficient dose required to prevent secondary cancer. Additionally, there was very little toxic effect demonstrated in a previous study employing ACR at 80 mg/kg/day for 20 weeks [12]. The data from the preliminary study could support the fact that the immunosuppressive or anti-cancer

effect of ACR when administered at a dose of 100 mg/kg/day is not due to toxic effects but to bio-activity.

In addition to the non-promotive effect of ACR on cancer proliferation, the augmentation of IFN- γ expression in spleen lymphocytes by ACR would support its potential use in a clinical environment. It is well known that HCC is closely linked to viral hepatitis, such as Hepatitis B or C. The action of IFN- γ , a representative cytokine that possesses anti-viral activity through its effect on replication, may provide great advantages associated with the clinical use of ACR [34–36].

In this study, we showed that ACR administered orally at 100 mg/kg/day had an almost equivalent immunosuppressive effect as CsA administered subcutaneously by injection at 1 mg/kg/day. Although ACR is a promising chemopreventive drug for use in HCC, ACR exerts its effect only after long periods of administration. Therefore, we believe our new findings concerning host immunity could contribute significantly towards its potential clinical use.

Acknowledgements

We would like to thank Mrs. Yasuko Sakuma, Ms. Megumi Hata and Ms. Harumi Kawana for their skillful technical assistance.

This study was supported by a grant to T.M. from the Health and Labor Science Research Grants from the Ministry of Health, Labor and Welfare (Research on Biological Resources) and by a grant from the "Strategic Research Platform" for Private Universities: matching fund subsidy from MEXT.

References

- [1] Dresser DW. Adjuvanticity of vitamin A. *Nature* 1968;217:527–9.
- [2] Floersheim GL, Bollag W. Accelerated rejection of skin homografts by vitamin A acid. *Transplantation* 1972;14:564–7.
- [3] Dennert G, Lotan R. Effects of retinoic acid on the immune system: stimulation of T killer cell induction. *Eur J Immunol* 1978;8:23–9.
- [4] Malkovsky M, Edwards AJ, Hunt R, Palmer L, Medawar PB. T-cell-mediated enhancement of host-versus-graft reactivity in mice fed a diet enriched in vitamin A acetate. *Nature* 1983;302:338–40.
- [5] Kirkman RL, Barrett LV, Carter P, Reed MH, Shapiro ME. RO 23-6457 prolongs survival of vascularized allografts in rodents and primates. *J Surg Res* 1990;48:304–7.
- [6] Kiss E, Adams J, Grone HJ, Wagner J. Isotretinoin ameliorates renal damage in experimental acute renal allograft rejection. *Transplantation* 2003;76:480–9.
- [7] Seino K, Yamauchi T, Shikata K, Kobayashi K, Nagai M, Taniguchi M, et al. Prevention of acute and chronic allograft rejection by a novel retinoic acid receptor- α -selective agonist. *Int Immunol* 2004;16:665–73.
- [8] Adams J, Kiss E, Arroyo AB, Bonrouhi M, Sun Q, Li Z, et al. 13-cis retinoic acid inhibits development and progression of chronic allograft nephropathy. *Am J Pathol* 2005;167:285–98.
- [9] Muto Y, Moriwaki H, Ninomiya M, Adachi A, Saito K, Takasaki KT, et al. Prevention of second primary tumors by an acyclic retinoid, polyphenolic acid, in patients with hepatocellular carcinoma. Hepatoma Prevention Study Group. *N Engl J Med* 1996;334:1561–7.
- [10] Suzui M, Masuda M, Lim JT, Albanese C, Pestell RG, Weinstein IB. Growth inhibition of human hepatoma cells by acyclic retinoid is associated with induction of p21 (CIP1) and inhibition of expression of cyclin D1. *Cancer Res* 2002;62:3997–4006.
- [11] Matsushima-Nishiwaki R, Okuno M, Takano Y, Kojima S, Friedman SL, Moriwaki H. Molecular mechanism for growth suppression of human hepatocellular carcinoma cells by acyclic retinoid. *Carcinogenesis* 2003;24:1353–9.
- [12] Kagawa M, Sano T, Ishibashi N, Hashimoto M, Okuno M, Moriwaki H, et al. An acyclic retinoid, NIK-333, inhibits N-diethylnitrosamine-induced rat hepatocarcinogenesis through suppression of TGF- α expression and cell proliferation. *Carcinogenesis* 2004;25:979–85.
- [13] Shao RX, Otsuka M, Kato N, Taniguchi H, Hoshida Y, Moriyama M, et al. Acyclic retinoid inhibits human hepatoma cell growth by suppressing fibroblast growth factor-mediated signaling pathways. *Gastroenterology* 2005;128:86–95.
- [14] Tsuchiya H, Akechi Y, Ikeda R, Nishio R, Sakabe T, Terabayashi K, et al. Suppressive effects of retinoids on iron-induced oxidative stress in the liver. *Gastroenterology* 2009;136:341–50.
- [15] Komi Y, Sogabe Y, Ishibashi N, Sato Y, Moriwaki H, Shimokado K, et al. Acyclic retinoid inhibits angiogenesis by suppressing the MAPK pathway. *Lab Invest* 2009;90:52–60.
- [16] Altucci L, Gronemeyer H. The promise of retinoids to fight against cancer. *Nat Rev Cancer* 2001;1:181–93.
- [17] Chen Q, Ross AC. Inaugural Article: Vitamin A and immune function: retinoic acid modulates population dynamics in antigen receptor and CD38-stimulated splenic B cells. *Proc Natl Acad Sci USA* 2005;102:14142–9.
- [18] Inoue Y, Kashima Y, Aizawa K, Hatakeyama K. A new rat colon cancer cell line metastasizes spontaneously: biologic characteristics and chemotherapeutic response. *Jpn J Cancer Res* 1991;82:90–7.
- [19] Ohsawa I, Murakami T, Uemoto S, Kobayashi E. In vivo luminescent imaging of cyclosporin A-mediated cancer progression in rats. *Transplantation* 2006;81:1558–67.
- [20] Olausson M, Mjornstedt L, Lindholm L, Brynner H. Non-suture organ grafting to the neck vessels in rats. *Acta Chir Scand* 1984;150:463–7.
- [21] Kamada N, Calne RY. Orthotopic liver transplantation in the rat. Technique using cuff for portal vein anastomosis and biliary drainage. *Transplantation* 1979;28:47–50.
- [22] Chambon P. A decade of molecular biology of retinoic acid receptors. *FASEB J* 1996;10:940–54.
- [23] Lotan R. Retinoids in cancer chemoprevention. *FASEB J* 1996;10:1031–9.
- [24] Medawar PB, Hunt R. Anti-cancer action of retinoids. *Immunology* 1981;42:349–53.
- [25] Malkovsky M, Hunt R, Palmer L, Dore C, Medawar PB. Retinyl acetate-mediated augmentation of resistance to a transplantable 3-methylcholanthrene-induced fibrosarcoma. The dose response and time course. *Transplantation* 1984;38:158–61.
- [26] Murakami K, Sakukawa R, Sano M, Hashimoto A, Shibata J, Yamada Y, et al. Inhibition of angiogenesis and intrahepatic growth of colon cancer by TAC-101. *Clin Cancer Res* 1999;5:2304–10.
- [27] Yokoyama I, Carr B, Saitsu H, Iwatsuki S, Starzl TE. Accelerated growth rates of recurrent hepatocellular carcinoma after liver transplantation. *Cancer* 1991;68:2095–100.
- [28] Freise CE, Ferrell L, Liu T, Ascher NL, Roberts JP. Effect of systemic cyclosporine on tumor recurrence after liver transplantation in a model of hepatocellular carcinoma. *Transplantation* 1999;67:510–3.
- [29] Hojo M, Morimoto T, Maluccio M, Asano T, Morimoto K, Lagman M, et al. Cyclosporine induces cancer progression by a cell-autonomous mechanism. *Nature* 1999;397:530–4.
- [30] Guba M, von Breitenbuch P, Steinbauer M, Koehl G, Flegel S, Hornung M, et al. Rapamycin inhibits primary and metastatic tumor growth by antiangiogenesis: involvement of vascular endothelial growth factor. *Nat Med* 2002;8:128–35.
- [31] Tange S, Scherer MN, Graeb C, Weiss T, Justl M, Frank E, et al. The antineoplastic drug Paclitaxel has immunosuppressive properties that can effectively promote allograft survival in a rat heart transplant model. *Transplantation* 2002;73:216–23.
- [32] Tanaka T, Takahara S, Hatori M, Suzuki K, Wang J, Ichimaru N, et al. A novel immunosuppressive drug, FTY720, prevents the cancer progression induced by cyclosporine. *Cancer Lett* 2002;181:165–71.
- [33] Ohsawa I, Uemoto S, Kobayashi E, Murakami T. Control of cyclosporine A-induced tumor progression using 15-deoxyspergualin for rat cardiac transplantation. *Transplantation* 2007;84:424–8.
- [34] Ross AC, Stephensen CB. Vitamin A and retinoids in antiviral responses. *FASEB J* 1996;10:979–85.
- [35] Bocher WO, Wallasch C, Hohler T, Galle PR. All-trans retinoic acid for treatment of chronic hepatitis C. *Liver Int* 2008;28:347–54.
- [36] Trotter C, Colombo M, Mann KK, Miller Jr WH, Ward BJ. Retinoids inhibit measles virus through a type I IFN-dependent bystander effect. *FASEB J* 2009;23:3203–12.

CD39/ENTPD1 Expression by CD4⁺Foxp3⁺ Regulatory T Cells Promotes Hepatic Metastatic Tumor Growth in Mice

XIAOFENG SUN,* YAN WU,* WENDA GAO,† KEIICHI ENJOJI,* EVA CSIZMADIA,* CHRISTA E. MÜLLER,§ TAKASHI MURAKAMI,|| and SIMON C. ROBSON*

Departments of *Medicine and †Surgery, Transplantation Institute, Beth Israel Deaconess Medical Center, Harvard Medical School, Boston, Massachusetts; §Pharmaceutical Institute, University of Bonn, Bonn, Germany; and ||Division of Bioimaging Sciences, Center for Molecular Medicine, Jichi Medical University, Shimotsuke, Tochigi, Japan

BACKGROUND & AIMS: Adenosine mediates immune suppression and is generated by the ectonucleotidases CD39 (ENTPD1) and CD73 that are expressed on vascular endothelial cells and regulatory T cells (Tregs). Although tumor-infiltrating immune cells include Foxp3⁺ Tregs, it is not clear whether local adenosine generation by Tregs promotes tumor growth in a CD39-dependent manner. In this study, we have examined the effect of CD39 expression by Tregs on effector immune cell responses to hepatic metastases in vivo. **METHODS:** A model of hepatic metastatic cancer was developed with portal vein infusion of luciferase-expressing melanoma B16/F10 cells and MCA38 colon cancer cells in wild-type (wt) and mutant mice null for *Cd39*. Chimeric mice were generated by bone marrow transplantation (BMT) using *Cd39* null or wt C57BL6 donors and irradiated recipient mice. **RESULTS:** We demonstrate that hepatic growth of melanoma metastatic tumors was strongly inhibited in mice with *Cd39* null vasculature or in wt mice with circulating *Cd39* null bone marrow-derived cells. We show functional CD39 expression on CD4⁺Foxp3⁺ Tregs suppressed antitumor immunity mediated by natural killer (NK) cells in vitro and in vivo. Finally, inhibition of CD39 activity by polyoxometalate-1, a pharmacologic inhibitor of nucleoside triphosphate diphosphohydrolase activity, significantly inhibited tumor growth ($P < .001$). **CONCLUSIONS: CD39 expression on Tregs inhibits NK activity and is permissive for metastatic growth. Pharmacologic or targeted inhibition of CD39 enzymatic activity may find utility as an adjunct therapy for secondary hepatic malignancies.**

Keywords: Ectonucleoside Triphosphate Diphosphohydrolase-1; Regulatory T Cell (Treg); Cancer Therapy; Liver.

Although advances in therapies for hepatic metastatic disease have occurred,^{1,2} limitations of vascular epithelial growth factor-based antiangiogenesis strategies and other regimens remain a major clinical problem. The tumor microenvironment may regulate local cellular responses by generating purinergic mediators that dampen antitumor immunity.³ The effects of extracellular nucleotides and nucleotides are mediated by type 1 purinergic receptors for adenosine and type 2 purinergic receptors that bind extracellular nucleotides.⁴ Adenosine may promote tumor growth by stimulating vascular endothelial cell proliferation and by inhibiting immune cell cytokine synthesis, trans-endothelium migration, and antitumor effector responses.^{3,5,6}

CD39/ENTPD1 (ectonucleoside triphosphate diphosphohydrolase-1) is the dominant ectonucleotidase expressed by endothelial cells and immune regulatory T cells (Tregs). CD39 drives the sequential hydrolysis of both adenosine triphosphate (ATP) and adenosine diphosphate (ADP) to adenosine monophosphate (AMP).⁷⁻¹⁰ AMP is further degraded by CD73/ecto-5'-nucleotidase to adenosine. CD39 expression by the vasculature is an absolute requirement for tumor angiogenesis.¹¹ We have noted that deletion of *Cd39* on Tregs results in heightened alloimmune responses.⁹ Whether CD39 expression by tumor-infiltrating immune cells facilitates tumor growth has not been explored to date.

Melanoma and colon cancers are aggressive, lethal tumors that often target the liver. In this study, we note that in our model antitumor activity depends on natural killer (NK) cells. CD4⁺Foxp3⁺ Tregs inhibit NK cell-mediated antitumor functions, a pathway that depends on intrinsic CD39 expression. Pharmacologic inhibition of CD39, using POM-1 (polyoxometalate-1),¹² likewise inhibits tumor growth. These findings suggest that targeted inhibition of CD39 might find utility as an adjunct therapy for metastatic hepatic malignancy.

Melanoma and colon cancers are aggressive, lethal tumors that often target the liver. In this study, we note that in our model antitumor activity depends on natural killer (NK) cells. CD4⁺Foxp3⁺ Tregs inhibit NK cell-mediated antitumor functions, a pathway that depends on intrinsic CD39 expression. Pharmacologic inhibition of CD39, using POM-1 (polyoxometalate-1),¹² likewise inhibits tumor growth. These findings suggest that targeted inhibition of CD39 might find utility as an adjunct therapy for metastatic hepatic malignancy.

Abbreviations used in this paper: ADP, adenosine diphosphate; AMP, adenosine monophosphate; ATP, adenosine triphosphate; BMT, bone marrow transplantation; DNAM-1, DNAX accessory molecule-1; ENTPD1, ectonucleoside triphosphate diphosphohydrolase-1; FACS, fluorescence-activated cell sorting; GFP, green fluorescent protein; IFN- γ , interferon- γ ; NK, natural killer; NTPDase, nucleoside triphosphate diphosphohydrolase; PE, phycoerythrin; POM-1, polyoxometalate-1; TCR β , T-cell receptor β ; TGF- β , transforming growth factor- β ; TLC, thin-layer chromatography; Treg, regulatory T cell; wt, wild-type.

© 2010 by the AGA Institute

0016-5085/\$36.00

doi:10.1053/j.gastro.2010.05.007

Materials and Methods

Animals

Six- to 14-week-old male C57BL6 *Cd39* null mice were used.⁸ Age-, sex-, and strain-matched wild-type (wt) mice and (γ c)/*Rag2*^{-/-} mice were purchased from Taconic Farms (Germantown, NY). *Rag1*^{-/-} mice were from The Jackson Laboratory (Bar Harbor, ME). Foxp3-GFP (green fluorescent protein) knock-in mice were generated as described.¹³

Animal Experimentation Protocols were reviewed and approved by the Institutional Animal Care and Use Committees of Beth Israel Deaconess Medical Center.

Antibodies and Reagents

All chemicals were obtained from Sigma-Aldrich (St Louis, MO). Fluorescence-activated cell sorting (FACS) studies were performed with the use of fluorescein isothiocyanate-, phycoerythrin (PE)-, Cy-chrome-, or allophycocyanin-conjugated antibodies. The following antibodies used for FACS and analysis were from eBioscience

(San Diego, CA): antimouse CD3 (clone: eBio500A2), CD4 (GK1.5), CD8 (53-6.7), CD28 (37.51), CD39 (24DMS1), T-cell receptor β (TCR β ; H57-597), and NK1.1 (PK136) (BD Bioscience, San Jose, CA). FACS data were analyzed with FlowJo software (TreeStar Inc, Ashland, OR). Antibodies used for immunohistochemistry were the following: CD31, CD4, CD8, CD11b, Gr-1 (LY6C and LY6G; BD Bioscience), F4/80, Thy1.2, Foxp3, NKp46 (R&D Systems, Minneapolis, MN), and polyclonal rabbit anti-mouse CD39 antibody.¹⁴ Anti-PE MicroBeads and anti-Biotin MACSiBead Particles were from Miltenyi Biotec Inc (Auburn, CA). Nucleoside triphosphate diphosphohydrolase (NTPDase) inhibitor POM-1 was obtained as described.¹²

Isolation of Spleen and Lymph Node Tregs, NK Cells, and Cytotoxicity Assay

Lymphocytes were positively selected with the use of MOFLO or FACSAria cell sorter (BD Bioscience, San Jose, CA) producing >99% cell population. NK cells were

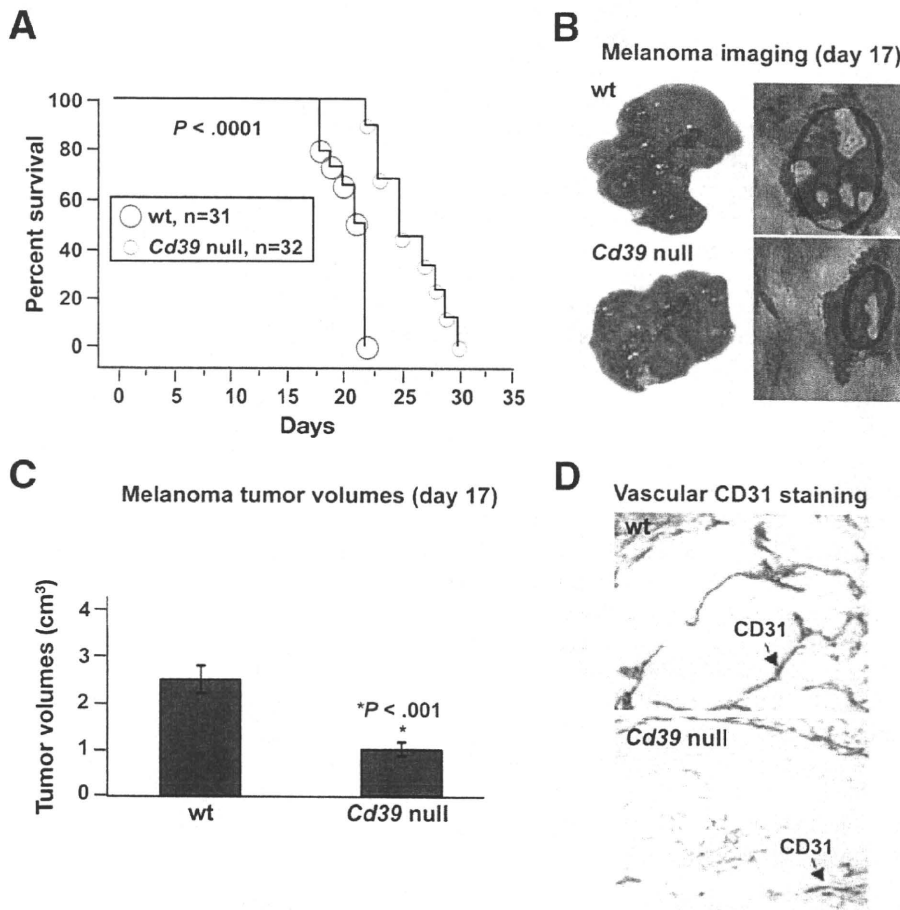


Figure 1. *Cd39* deletion inhibits metastatic melanoma growth in livers. (A) Survival and/or time to euthanasia in tumor-bearing mice after luc-B16/F10 cell infusion (1.5×10^5 cells) through the portal vein ($P < .0001$). (B) Representative images of tumor-bearing livers on day 17 (left panel) and in vivo bioluminescent imaging of tumor metastasis (right panel). (C) Tumor volumes at day 17 ($*P < .001$). (D) Representative immunohistochemical staining in tissue sections obtained from (B) using anti-CD31 (a marker for endothelium) antibody (magnification $\times 400$). Data are given as means \pm SEMs.

sorted as NK1.1⁺TCR β ⁻ cells, and Tregs were sorted as CD4⁺GFP⁺ cells with the use of Foxp3-GFP knock-in mice.¹³ Cytolytic activity of NK cells was tested at a number of effector-to-target ratios against N YAC-1 cells with the use of the LIVE/DEAD Cell-Mediated Cytotoxicity Kit (Invitrogen Life Technologies, Carlsbad, CA).

Tumor Cell Lines

Luciferase-expressing B16/F10 (luc-B16/F10 on BL6) cells were developed as described.¹⁵ Syngeneic murine MCA38 colon cancer cells provided by Dr Nicholas P. Restifo (National Cancer Institute) were maintained in RPMI 1640 medium supplemented with 10% fetal calf serum and glutamine. YAC-1 cells were purchased from American Type Culture Collection (Manassas, VA).

Tumor Cell Inoculation and In Vivo Bioluminescence Imaging

Luc-B16/F10 and MCA38 cells were harvested by trypsinization and resuspended with Hanks' balanced salt solution/2% fetal bovine serum for injection. Luc-B16/F10 cells (1.5×10^5 cells for standard and bone marrow transplantation [BMT] experiments, and 2×10^5 cells for adoptive transfer experiments) and MCA38 cells (1.0×10^5 cells for all experiments except 2×10^5 cells for POM-1 treatments) were infused into liver through the portal vein. Tumor-bearing mice were killed and examined for tumor growth at indicated time points or if any distress or suffering was observed. In vivo tumor progression was examined with the use of the noninvasive bioimaging system IVIS (Xenogen, San Francisco, CA), as described previously,¹⁵ at the Longwood Small Animal Imaging Facility. Perpendicular tumor diameters were also directly measured, and tumor volume was determined by integration with the following formula: $\Sigma t_1 + t_2 + \dots + t_n$ ($t = a^2 \times b \times 0.52$; $a =$ smaller tumor diameter, $b =$ larger tumor diameter).^{6,16}

Bone Marrow Transplantation

Six-week-old male *Cd39* null mice and wt mice were exposed to 10 Gy (0.28 Gy/min, 200 kV, 4 mA) γ -ray total body irradiation, using an Andrex Smart 225 (Andrex Radiation Products AS, Copenhagen, Denmark) with a 4-mm aluminum filter. The marrow from the femur and tibia of matched *Cd39* null mice and wt mice was harvested, and cells were purified under sterile conditions. Irradiated recipient mice received 10×10^6 bone marrow cells intravenously. The success of BMT was validated by FACS analysis of immune cell populations (not shown). Mice that received a transplant were housed in autoclaved cages for 8 weeks before experimentation.¹⁷

Adoptive Transfer Experiments

Freshly sorted CD4⁺ T cells (1×10^6), CD8⁺ T cells (0.5×10^6), Treg cells (0.1×10^6), or Teff cells (0.9×10^6) from *Cd39* null or wt mice or wt NK cells (1.5×10^6)

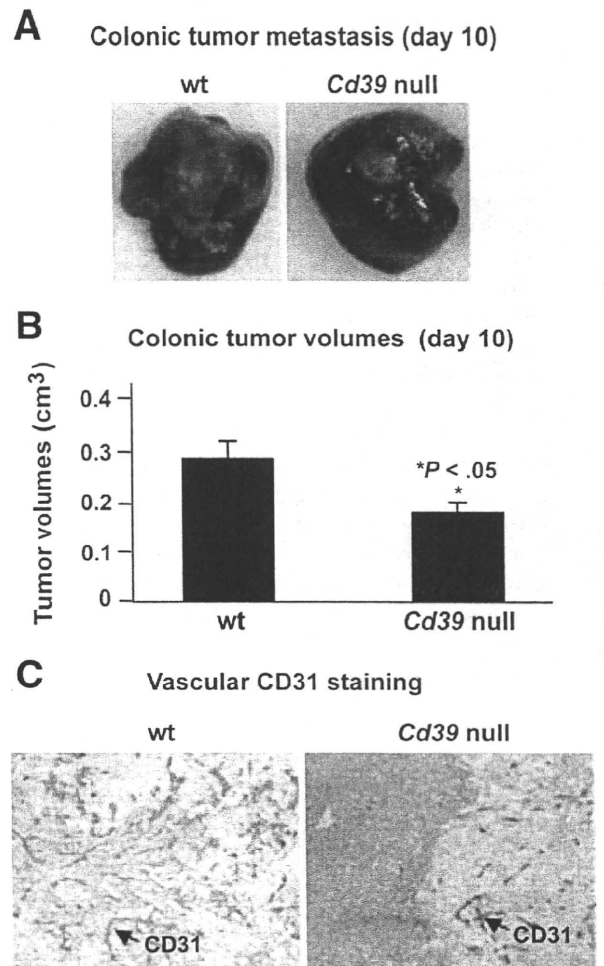


Figure 2. *Cd39* deletion inhibits metastatic colon tumor growth in livers. (A) Representative images of tumor-bearing livers at day 10 after portal vein infusion of 1.0×10^5 MCA38 cells. (B) Tumor volumes at day 10 (**P* < .05). (C) Immunohistochemical staining on tissue sections obtained from (A) using anti-CD31 (a marker for endothelium) antibody (magnification $\times 400$). Data are given as means \pm SEMs.

were injected into Rag1^{-/-} mice. Wt NK cells (1×10^6), alone or with wt Tregs (1×10^6), or *Cd39* null Tregs (1×10^6) were injected into (γ c)/Rag2^{-/-} mice.

Histology and Immunohistochemistry

Paraffin-embedded or frozen sections of tumor-bearing livers were analyzed by immunohistochemical staining as described.^{11,18} Apoptosis was determined with the use of TdT (terminal deoxynucleotidyl-transferase)-mediated nick-end labeling staining (Millipore, Temecula, CA).

Measurement of IFN- γ Production by Enzyme-Linked Immunoabsorbent Assay

Interferon- γ (IFN- γ) plasma concentrations were measured with the use of the Mouse IFN- γ (Femato-HS) ELISA Ready-To-Go kit from eBioscience.

Purification of Tumor- or Liver-Infiltrating Mononuclear Cells

These cells were purified as described previously.¹⁹

Thin-Layer Chromatography Analysis

NTPDase activity of CD39 on freshly isolated cells was analyzed with the use of thin-layer chromatography (TLC), as described.^{9,19}

Statistical Analysis

Results in this study are expressed as means \pm SEMs of values (obtained from ≥ 4 mice per group and/or ≥ 3 independent in vitro experiments). All histology and immunohistochemical images are representative of ≥ 4 mice per group.

For statistical analyses, the 2-tailed Student *t* test was used. Animal time to euthanasia was analyzed with the Kaplan–Meier method and was compared with the log-rank test (StatView 5.0 analysis software; SAS Institute, Cary, NC). Significance was defined as $P < .05$.

Results

CD39 Expression Facilitates Tumor Growth

Portal vein infusion of luciferase-expressing melanoma B16/F10 (luc-B16/F10) cells and MCA38 colon cancer cells resulted in cells being retained in liver sinusoids; no tumors were found in lungs or other sites within 14 days (data not shown). Melanoma-bearing *Cd39* null mice had longer times to euthanasia and death than the wt mice ($P < .0001$; Figure 1A).

Tumor growth in liver was substantially inhibited in *Cd39* null mice (melanoma data in Figure 1B and C and colonic tumor studies in Figure 2A and B) and were associated with decreased angiogenesis (Figure 1D and Figure 2C). Luc-B16/F10 cells and MCA38 cells do not express CD39 per se in vitro or in vivo at any tumor progression stages (data not shown). Hence, endogenous CD39 expression is required for the development of metastatic tumors in the liver.

We next studied bone marrow reconstitution. Melanoma growth was significantly delayed in the livers of irradiated, reconstituted wt mice that had received *Cd39* null BM transplant (Figure 3A and B; $P < .05$), compared with wt mice that received wt BM transplant. Here, defective angiogenesis in tumors was associated with *Cd39* null vasculature. High levels of cell death were clearly demonstrated at the center of tumor nodules (Figure 3C).

Differences of hepatic melanoma growth among groups on days 14 and 21 were comparable to that seen on day 10 (Supplementary Figure 1; data not shown). Mortality was only seen in wt BM-wt mice, from day 17; all other groups survived for ≥ 21 days (data not shown). Taken together, these data indicate that CD39 expression by BM-derived cells is critical for tumor growth.

Characterization of Tumor-Infiltrating Cells

Melanoma tumor tissues were infiltrated by CD39⁺, CD4⁺, CD8⁺, and Thy1.2⁺ cells; macrophages (F4/80⁺); granulocytes and leukocytes (Gr-1⁺); NK (NK1.1⁺TCR β ⁻) and NKT (NK1.1⁺TCR β ⁺) cells; as well as cells positive for CD11b, indicative of myeloid-derived suppressive cells (Supplementary Figure 2A and B).²⁰

A proportion of the infiltrating CD4⁺ cells was positive for both CD39 and Foxp3 (Supplementary Figure 2C and D), suggesting that Tregs infiltrate tumors.^{13,21} Because Tregs express CD39 (Supplementary Figure 2C and D),⁹ we measured ecto-ADPase activity of purified tumor-infiltrating mononuclear cells by TLC assay. *Cd39* null cells exhibited markedly decreased ecto-ADPase activity (Figure 3D).

Cd39 Null CD4⁺ T Cells Inhibit Tumor Growth

Immunity to melanoma could be mediated by a variety of immune cells (eg, NK, NKT, and CD8⁺ T cells).^{15,22–25} Tregs have been shown to suppress antimelanoma cytotoxic responses by CD8⁺ cytotoxic T lymphocytes, NKT cells, and NK cells at the local tumor site.^{15,22,23,26}

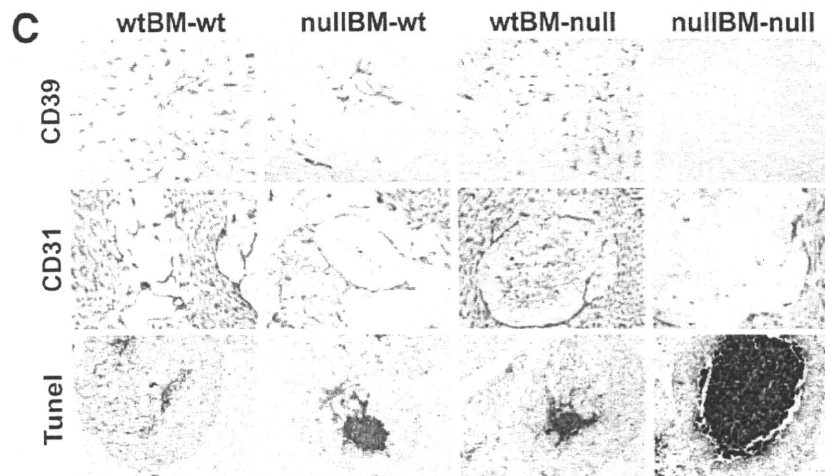
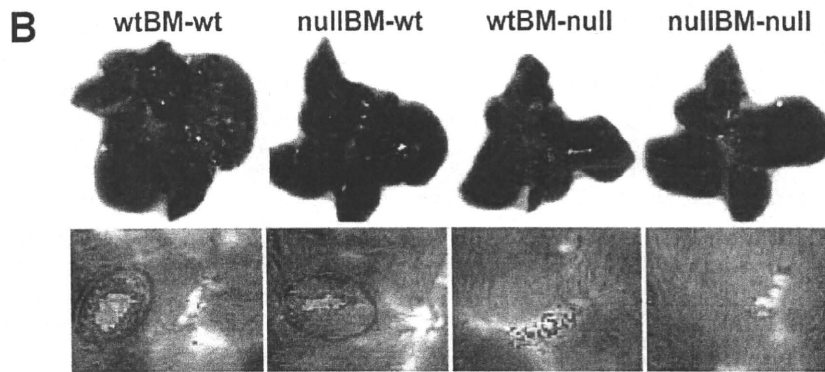
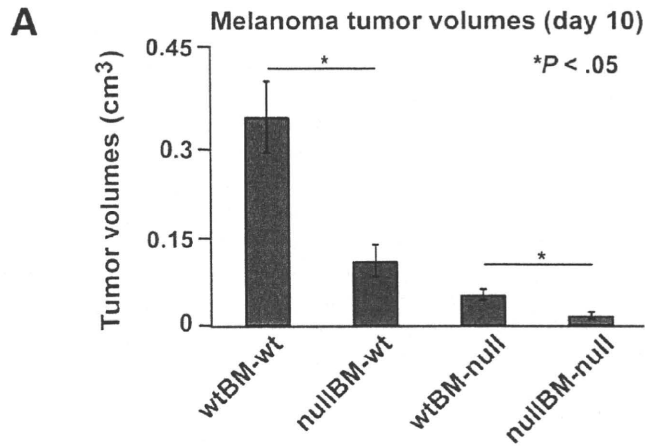
To examine first whether CD39 expression on CD4⁺ T cells is involved in antitumor immunity, wt or *Cd39* null CD4⁺ T cells in combination with effector wt CD8⁺ T cells were adoptively transferred into Rag1^{-/-} mice. CD8⁺ T cells alone failed to control melanoma growth unless CD4⁺ T cells were co-transferred (Figure 4A). Tumor growth was significantly inhibited when Rag1^{-/-} mice were co-transferred with *Cd39* null CD4⁺ T cells, compared with wt CD4⁺ T cells ($P < .05$; Figure 4A).

Liver-infiltrating mononuclear cells of these mice were isolated, and the percentages of CD4⁺, CD8⁺, NK, and NKT cells were evaluated by FACS analysis (Figure 4B). Heightened levels of NK cells were observed in mice adoptively transferred with *Cd39* null CD4⁺ T cells (wtCD4⁺wtCD8, 23.25% \pm 5.24% vs nullCD4⁺wtCD8, 34.34% \pm 8.18%; $P = .05$). In contrast, percentages of adoptively transferred CD4⁺ or CD8⁺ cells remained at the same level (Figure 4B).

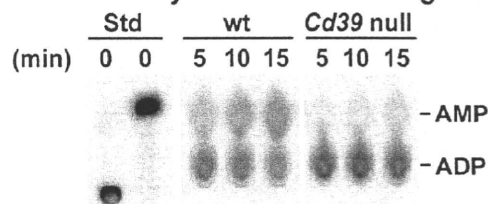
We next transferred wt or *Cd39* null CD4⁺ T cells into Rag1^{-/-} mice followed by subcutaneous injection of 0.2 mL of Matrigel into the flanks 24 hours later. We did not observe any inhibition by CD4⁺ T cells on the process of endothelial angiogenesis (Supplementary Figure 3).

NK Cells Mediate Antitumor Immunity

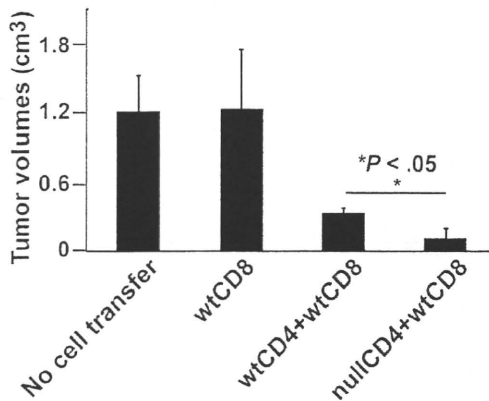
We next performed similar adoptive transfer experiments with the use of NK cell-deficient (γ c)/Rag2^{-/-} mice, instead of Rag1^{-/-} mice. In (γ c)/Rag2^{-/-} mice, no inhibition of melanoma growth was noted even after T-cell transfer (Figure 5A), suggesting that NK cells are required to inhibit melanoma growth. We next reconstituted (γ c)/Rag2^{-/-} mice with wt NK cells followed by melanoma cell



D Ecto-ADPase activity of tumor infiltrating mononuclear cells



A Rag1^{-/-} mice adoptively transferred with T cells



B Rag1^{-/-} mice adoptively transferred with T cells

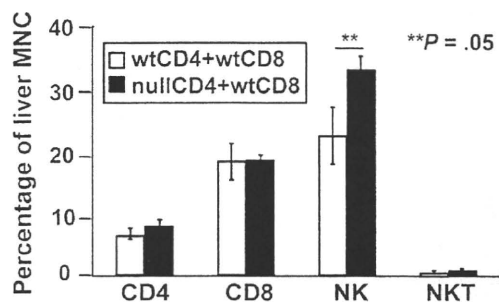


Figure 4. *Cd39* null *CD4*⁺ T cells inhibit tumor growth. (A) Tumor volumes of tumor-bearing Rag1^{-/-} mice adoptively transferred with lymphocytes (*CD4*⁺ T cells, 1×10^6 ; *CD8*⁺ T cells, 0.5×10^6), followed by portal vein infusion of 2×10^5 luc-B16/F10 cells, on day 14. (B) Percentage of *CD4*⁺, *CD8*⁺, NK1.1⁺, and NKT lymphocytes of liver mononuclear cells isolated from tumor-bearing livers above. Data are given as means \pm SEMs. * $P < .05$, ** $P = .05$.

inoculation. NK-cell reconstitution greatly suppressed tumor growth in (γ c)/Rag2^{-/-} mice ($P < .001$; Figure 5B), with migration of NK cells into the liver ($P < .001$; Figure 5C) expressing Nkp46 (Figure 5D). Antitumor activity of NK cells was noted to depend on cell number (data not shown). Colonic tumor growth was also inhibited in Rag1^{-/-} mice, compared with (γ c)/Rag2^{-/-} mice ($P < 1E-06$; Supplementary Figure 4A and B), associated with migration of endogenous NK cells into the liver ($P < 1E-06$; Supplementary Figure 4C) and strong expression of Nkp46

(Supplementary Figure 4D). These data indicate that NK cells play important roles in antitumor immunity.

Tregs Suppress NK Cell-Mediated Antitumor Responses in a *CD39*-Dependent Manner

NK cell-mediated antitumor functions may be suppressed by Tregs in vitro and in vivo.^{22,26} This regulation seems NKG2D mediated and transforming growth factor- β (TGF- β) dependent.^{22,26,27} Extracellular purinergic mediators and related metabolites may also exert inhibitory effects on cytotoxic activity and cytokine production of activated NK cells.^{28,29} Therefore, it is conceivable that *CD39* expressed by Tregs regulates NK cell activity.

To test for this possibility, wt or *Cd39* null Tregs were activated with anti-*CD3*/*CD28* and interleukin-2 (IL-2) for 72 hours before coculturing with wt NK cells in vitro. We demonstrated specific ability of in vitro-activated Tregs to suppress NK cell-mediated cytotoxicity of YAC-1 target cells ($P < .01$, wtNK vs wtNK⁺wtTreg; Figure 6A). *Cd39* null Tregs lacked inhibitory effects on NK cell-mediated cytotoxicity (Figure 6A).

Rag1^{-/-} mice were then adoptively transferred with wt Tregs (*CD4*⁺GFP⁺Foxp3⁺) from Foxp3-GFP knock-in mice or with wt Teff (*CD4*⁺GFP⁻Foxp3⁻) or in combination, followed by melanoma cell inoculation. Decreased numbers of liver endogenous NK cells and lower plasma levels of IFN- γ were noted in mice transferred with Tregs alone, compared with mice transferred with Teff alone ($P < .05$ and $P < .01$, respectively) (Figure 6B and C). Effects of Tregs were dominant, as shown in Treg + Teff combinations (Figure 6B and C).

We reconstituted (γ c)/Rag2^{-/-} mice with wt NK cells alone or in combination with wt or *Cd39* null Treg, followed by melanoma cell inoculation. As expected, wt NK cells inhibited tumor growth. NK cells lost antitumor efficacy if co-transferred with wt Tregs. NK cell activity was preserved when *Cd39* null Tregs were co-transferred, with tumor growth abrogated ($P < .05$) (Figure 6D). Antitumor activity correlated with intrahepatic enrichment of administered NK cells (Figure 6E). Hence, Tregs directly suppress NK cell-controlled tumor expansion in a manner dependent on Treg-specific *CD39*.

Pharmacologic Inhibition of *CD39* Activity Impedes Tumor Growth

A high proportion of tumor-infiltrating *CD4*⁺ T cells are Foxp3⁺ Tregs. Deleting these suppressors or

Figure 3. *CD39* expression on bone marrow-derived cells facilitates tumor growth. Wild type (wt) and *Cd39* null (null) chimeric mice were generated by BMT (donor genotype designated first/recipients second). Eight weeks after BMT, 1.5×10^5 luc-B16/F10 cells were infused through the portal vein. (A) Tumor volumes on day 10 ($n = 6-8$ mice per group). (B) Representative images of tumor-bearing livers at day 10 (top) and in vivo bioluminescent imaging of tumor metastasis (bottom). (C) Representative immunohistochemical staining with the use of anti-*CD39* and anti-*CD31* antibodies and TdT (terminal deoxynucleotidyl-transferase)-mediated nick-end labeling staining for apoptosis (magnification $\times 400$ for *CD39*; $\times 200$ for *CD31* and TUNEL staining). (D) Ecto-ADPase activity in tumor-infiltrating mononuclear cells. Tumor-infiltrating mononuclear cells were isolated from tumor tissues of wt and *Cd39* null tumor-bearing mice. Thin-layer chromatography (TLC) analysis of ADP hydrolysis to AMP with the use of 1.5×10^5 cells was analyzed. Data are given as means \pm SEMs. * $P < .05$.

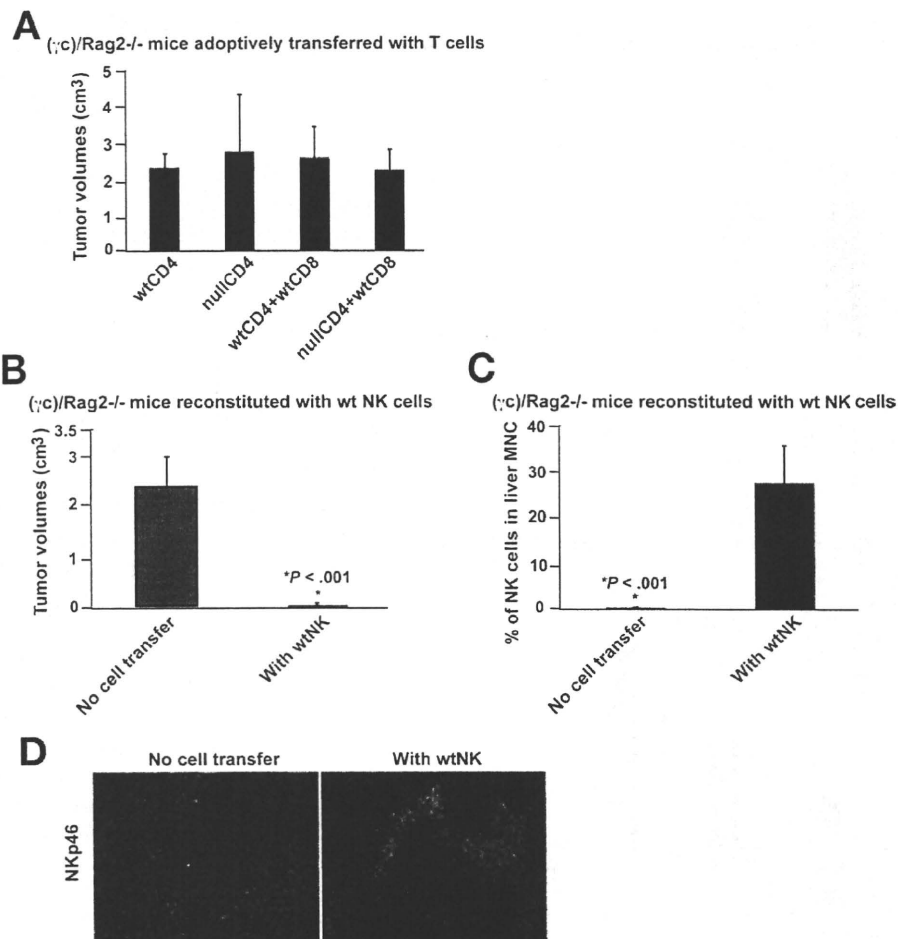


Figure 5. NK cells mediate antitumor immunity to melanoma. (A) Tumor volumes of tumor-bearing (γc)/Rag2^{-/-} mice adoptively transferred with lymphocytes (CD4⁺ T cells, 1×10^6 ; CD8⁺ T cells, 0.5×10^6), followed by portal vein infusion of 2×10^5 luc-B16/F10 cells, on day 14. (B) Tumor volumes of tumor-bearing (γc)/Rag2^{-/-} mice reconstituted with 1.5×10^6 of wt, spleen- and lymph node-derived NK cells (sorted as NK1.1⁺TCR β ⁻ using MOFLO), on day 14. (C) Percentage of NK cells among mononuclear cells isolated from tumor-bearing livers of *panel B*. (D) Immunofluorescence staining with the use of anti-NKp46 antibody on livers of *panel B*. DAPI staining nuclei in blue and NKp46 in red (magnification $\times 200$). Data are given as means \pm SEMs. * $P < .001$.

mitigating suppressive activity could boost antitumor immunity. Pharmacologic inhibition of CD39 enzymatic activity might be an anticancer treatment. POMs are anionic complexes that inhibit NTPDase activity¹² and have been proposed as chemotherapeutic agents against many human cancers, eg, colon cancer, lung cancer, and breast cancer.^{30,31}

We observed that POM-1 inhibited ecto-NTPDase activity of Tregs in vitro (Figure 7A). POM-1 (5 or 10 mg/kg/d) was then injected intraperitoneally into wt mice for 10 days after melanoma cell challenge. Tumor growth on day 14 decreased in POM-1-treated wt mice, in contrast to saline-treated wt mice ($P < .001$; Figure 7B). No detectable liver and renal toxicity was observed at suppressive doses (Supplementary Figure 5). In parallel, POM-1 (5 mg/kg/d) did not affect melanoma tumor growth in *Cd39* null mice, indicating that inhibitory

effects of POM-1 are mediated by CD39 ($P = .23$; Figure 7C). Furthermore, POM-1 (5 mg/kg/d) was shown to suppress hepatic metastatic colonic tumor growth in wt mice ($P < .05$; Figure 7D).

Discussion

We have already shown that CD39 expression on endothelium is important for angiogenesis and is required for tumor growth in the lung.^{11,18} We show now that infiltrating Tregs inhibit NK cell-mediated tumor cytotoxicity in a CD39-dependent manner in the liver. Tregs exhibit immunosuppressive effects on effector T cells, operational by adenosine-mediated pathways modulated by CD39 and CD73.⁹ Our current findings strengthen the notion that the expression of CD39 and

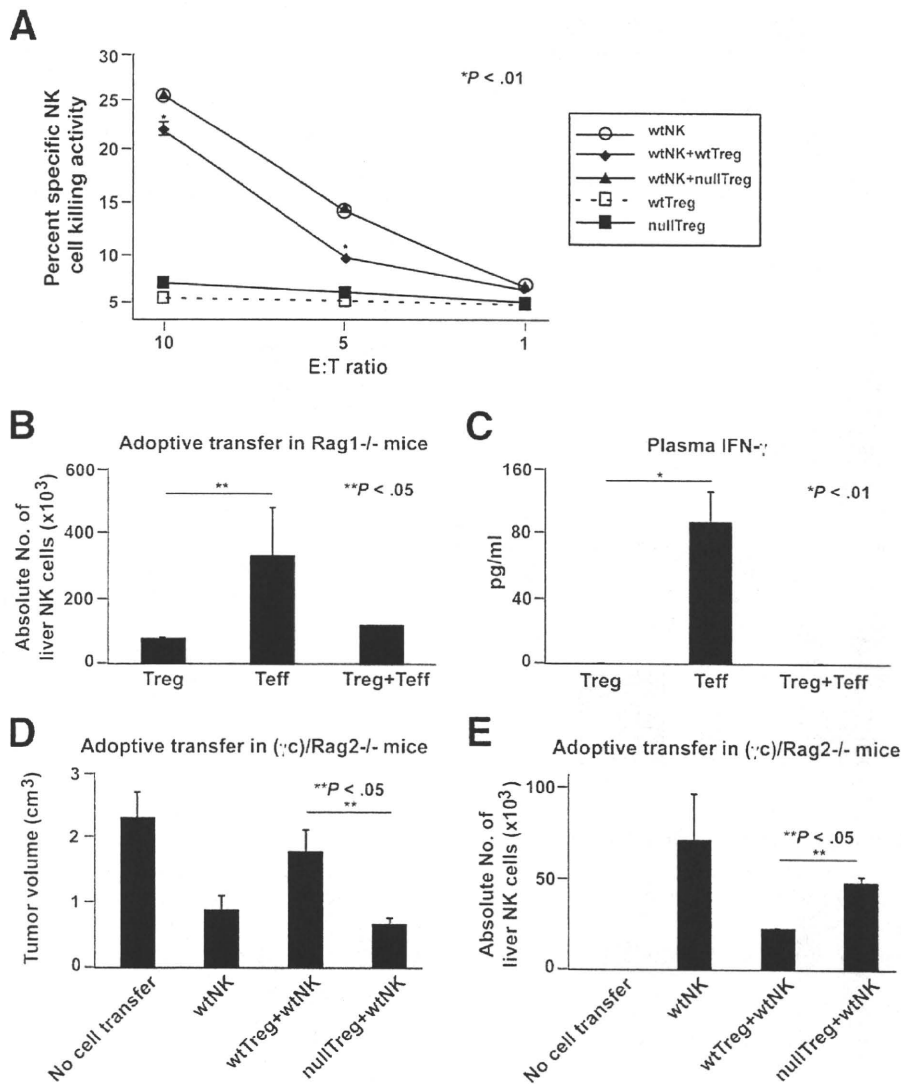


Figure 6. Tregs regulate NK cell-mediated antitumor immunity in a CD39-dependent manner. (A) *Cd39* null Tregs fail to suppress NK cell cytotoxicity in vitro. NK cells were cocultured at 1.5:1 and other ratios (not shown) with activated wt or *Cd39* null Tregs. The sorted CD4⁺GFP⁺ Tregs were stimulated with anti-CD3/CD28 bound MACS bead particles and interleukin-2 (100 ng/mL) for 72 hours before coculture. (**P* < .01, wtNK vs wtNK+wtTreg). (B) Absolute liver NK cell numbers in tumor-bearing Rag1^{-/-} mice adoptively transferred with sorted wt lymphocytes (Treg, 0.1 × 10⁶; Teff, 0.9 × 10⁶) as indicated, followed by portal vein infusion of 2 × 10⁵ luc-B16/F10 cells, on day 14. (C) Levels of IFN-γ in plasma obtained from mice in panel B. (D) Tumor volumes of tumor-bearing (γ)C/Rag2^{-/-} mice adoptively transferred with lymphocytes (Treg, 1.0 × 10⁶; NK, 1.0 × 10⁶), followed by portal vein infusion of 2 × 10⁵ luc-B16/F10 cells, on day 14. Mice received phosphate-buffered saline as controls. (E) Absolute liver NK cell numbers in tumor-bearing mice of panel D. Data are given as means ± SEMs. **P* < .01, ***P* < .05.

associated changes in nucleotide/nucleoside balance are integral components of Treg cell function.

NK cells are an important component of innate defenses against malignant cells. Tumor growth is accelerated in NK-deficient (γ)C/Rag2^{-/-} mice. This phenotype could be corrected by NK cell reconstitution. NK cell-mediated antitumor functions are susceptible to direct Treg suppression in vitro and in vivo.^{22,26,32} Suppression has been suggested to be, at least in part, NKG2D mediated and TGF-β dependent.^{22,26,27} However, other mechanisms might also be involved.³³

Adenosine interacts with 4 different adenosine receptor subtypes (A1, A2a, A2b, and A3 AR). A2a signaling has been shown to play a predominant role in inhibiting cytotoxicity of activated NK cells.^{6,28,34,35} A2b receptors have low affinity and might promote tumor growth at higher concentrations of adenosine.³⁶ Whether A2a and/or A2b are responsible for suppressing NK function in our model is currently undetermined.^{5,37}

NK cells express CD39, but lack CD73 expression.^{19,38} Several studies have reported that purines (ATP = ADP > AMP = adenosine) inhibit cellular proliferation, cytokine

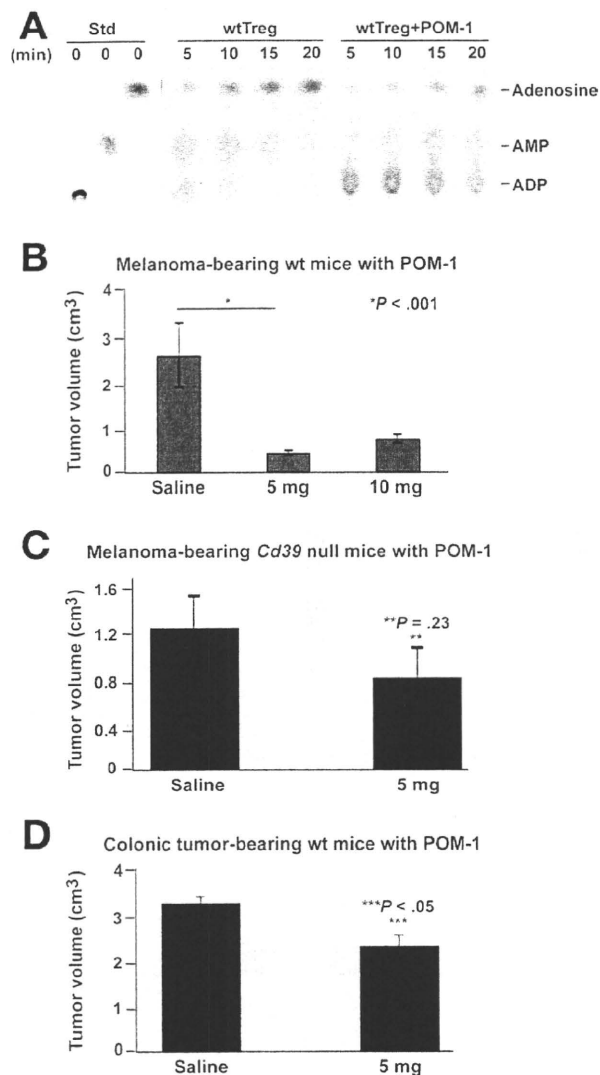


Figure 7. Pharmacologic inhibition of CD39 activity suppresses tumor growth. (A) Ecto-NTPDase activity of POM-1-treated wt Tregs in vitro. Wt Tregs (CD39⁺CD4⁺Foxp3⁺, 3×10^5) were pretreated with 26 μ m of POM-1, washed, and then subjected to TLC ADPase analysis. Tregs incubated in POM-1-free medium served as control. (B) Tumor volumes of melanoma-bearing wt mice (received 2×10^5 luc-B16/F10 cells) treated with POM-1 on a daily dosage of 5 or 10 mg/kg for 10 days, on day 14. Mice that received saline were used as controls. (C) Tumor volumes of melanoma-bearing *Cd39* null mice (received 2×10^5 luc-B16/F10 cells) treated with POM-1 on a daily dosage of 5 mg/kg for 10 days, on day 14. Mice that received saline served as controls. (D) Tumor volumes of colonic tumor-bearing wt mice (received 2×10^5 MCA38 cells) treated with POM-1 on a daily dosage of 5 mg/kg for 10 days, on day 14. Mice that received saline were used as controls. Data are given as means \pm SEMs. * $P < .001$, ** $P = .23$, *** $P < .05$.

production, and cytotoxic activity of activated NK cells.^{29,34,39–41} Molecular mechanisms underlying purine-mediated suppression of NK cell activity are highly complex. Whether and how deletion of *Cd39* affects NK cell activity may depend on the types of the stimuli and the

resulting balance between adenosine- and ATP/ADP-mediated signaling pathways and is being tested further.

Solid tumors are infiltrated by Tregs at a far higher frequency than seen in normal lymphoid organs. It is suggested that depleting Tregs with antibodies against surface markers, eg, CD25, would have a positive effect on the immunotherapy of cancer.⁴² Nevertheless, CD25 is also expressed on many types of activated immune cells, and benefits of this strategy are questionable. We show here that blocking CD39 enzymatic activity with POM-1, a pharmacologic inhibitor of NTPDase activity,¹² could inhibit adenosine generation by Tregs in vitro and abrogate tumor growth in vivo.

CD39 is also expressed on a variety of immune cells, including B cells, dendritic cells, macrophages, NK cells, NKT cells,^{9,19,35,43,44} and CD4⁺ T memory cells (CD4⁺CD44⁺CD62L⁻Foxp3⁻).⁴⁵ Tregs are also not the only tumor-infiltrating suppressor cells. Myeloid-derived suppressor cells have been shown to be potent suppressors of various T-cell functions in tumor-bearing mice and in patients with cancer.²⁰ In mice, these cells express myeloid-cell lineage differentiation antigens GR-1 and CD11b.²⁰ Monocyte and neutrophil populations express CD39,^{18,46,47} and it was shown here that tumor-infiltrating immune cells contain GR-1⁺ and CD11b⁺ cells (Supplementary Figure 2).

It was recently shown that B16/F10 melanoma cells express ligands for natural cytotoxicity receptors (NKp46 in mice) and DNAX accessory molecule-1 (DNAM-1), but not NKG2D.⁴⁸ Interference with both DNAM-1 and natural cytotoxicity receptor pathways results in dramatic decrease in killing of melanoma cells.⁴⁸ We have observed strong NKp46 staining on tumor-infiltrating NK cells, associated with decreased melanoma and colonic tumor growth (Figure 5 and Supplementary Figure 4).

NK cells may stimulate the maturation of dendritic cells,⁴⁹ produce cytokines that affect CD4⁺ and CD8⁺ effector T cells,⁵⁰ and regulate proliferation of T cells.⁵¹ Our current data clearly show that NK and Teff cells interact, particularly in the context of IFN- γ production, and that NK cells could directly influence adaptive immune responses.

We have noted effects of CD39 expression on pulmonary and subcutaneous metastases of melanoma, and colon and colorectal cancers (Beat Künzli and S.C.R., unpublished data, January 2008, and Jackson et al¹¹). Taken together, our studies provide an intriguing mechanism for the purinergic suppression of NK cell-mediated antitumor immunity by CD39 expression on Treg. Other investigators have recently shown that CD39 may be expressed on infiltrating T cells to generate adenosine in lymphoproliferative disorders⁵² or on Tregs associated with head and neck tumors.^{53,54} Work has been done also to neutralize tumor cell-expressed CD73 in a model of breast cancer with salutary effects.⁵⁵ Our work strongly

suggests that it is CD39 expression on Tregs that modulates NK cell reactivity against tumor cells.

Detailed analyses of CD39 expression and Treg function in patients at different stages of hepatic metastatic disease may help improve our understanding of the molecular mechanisms resulting in tumor growth and metastasis. Inhibition of CD39 expression and/or activity might also find future utility as a component of anticancer immunotherapy.

Supplementary Material

Note: To access the supplementary material accompanying this article, visit the online version of *Gastroenterology* at www.gastrojournal.org, and at doi: 10.1053/j.gastro.2010.05.007.

References

- Ogawa T, Takayama K, Takakura N, Kitano S, Ueno H. Anti-tumor angiogenesis therapy using soluble receptors: enhanced inhibition of tumor growth when soluble fibroblast growth factor receptor-1 is used with soluble vascular endothelial growth factor receptor. *Cancer Gene Ther* 2002;9:633–640.
- Chari RS, Helton WS, Marsh RD. Chemotherapy and regional therapy of hepatic colorectal metastases: expert consensus statement by Bartlett et al. *Ann Surg Oncol* 2006;13:1293–1295.
- Hoskin DW, Reynolds T, Blay J. Adenosine as a possible inhibitor of killer T-cell activation in the microenvironment of solid tumours. *Int J Cancer* 1994;59:854–855.
- Burnstock G. Purinergic signaling and vascular cell proliferation and death. *Arterioscler Thromb Vasc Biol* 2002;22:364–373.
- Spychala J. Tumor-promoting functions of adenosine. *Pharmacol Ther* 2000;87:161–173.
- Ohta A, Gorelik E, Prasad SJ, et al. A2A adenosine receptor protects tumors from antitumor T cells. *Proc Natl Acad Sci U S A* 2006;103:13132–13137.
- Plesner L. Ecto-ATPases: identities and functions. *Int Rev Cytol* 1995;158:141–214.
- Enyoji K, Sévigny J, Lin Y, et al. Targeted disruption of cd39/ATP diphosphohydrolase results in disordered hemostasis and thromboregulation. *Nat Med* 1999;5:1010–1017.
- Deaglio S, Dwyer KM, Gao W, et al. Adenosine generation catalyzed by CD39 and CD73 expressed on regulatory T cells mediates immune suppression. *J Exp Med* 2007;204:1257–1265.
- Borsellino G, Kleinewietfeld M, Di Mitri D, et al. Expression of ectonucleotidase CD39 by Foxp3+ Treg cells: hydrolysis of extracellular ATP and immune suppression. *Blood* 2007;110:1225–1232.
- Jackson SW, Hoshi T, Wu Y, et al. Disordered purinergic signaling inhibits pathological angiogenesis in cd39/Entpd1-null mice. *Am J Pathol* 2007;171:1395–1404.
- Müller CE, Iqbal J, Baqi Y, Zimmermann H, Rölllich A, Stephan H. Polyoxometalates—a new class of potent ecto-nucleoside triphosphate diphosphohydrolase (NTPDase) inhibitors. *Bioorg Med Chem Lett* 2006;16:5943–5947.
- Bettelli E, Carrier Y, Gao W, et al. Reciprocal developmental pathways for the generation of pathogenic effector TH17 and regulatory T cells. *Nature* 2006;441:235–238.
- Kaczmarek E, Koziak K, Sévigny J, et al. Identification and characterization of CD39/vascular ATP diphosphohydrolase. *J Biol Chem* 1996;271:33116–33122.
- Sato A, Ohtsuki M, Hata M, Kobayashi E, Murakami T. Antitumor activity of IFN- λ in murine tumor models. *J Immunol* 2006;176:7686–7694.
- Huang X, Wong MK, Yi H, et al. Combined therapy of local and metastatic 4T1 breast tumor in mice using SU6668, an inhibitor of angiogenic receptor tyrosine kinases, and the immunostimulator B7.2-IgG fusion protein. *Cancer Res* 2002;62:5727–5735.
- Day YJ, Huang L, McDuffie MJ, et al. Renal protection from ischemia mediated by A2A adenosine receptors on bone marrow-derived cells. *J Clin Invest* 2003;112:883–891.
- Goepfert C, Sundberg C, Sévigny J, et al. Disordered cellular migration and angiogenesis in cd39-null mice. *Circulation* 2001;104:3109–3115.
- Beldi G, Wu Y, Banz Y, et al. Natural killer T cell dysfunction in CD39-null mice protects against concanavalin A-induced hepatitis. *Hepatology* 2008;48:841–852.
- Gabrilovich DI, Nagaraj S. Myeloid-derived suppressor cells as regulators of the immune system. *Nat Rev Immunol* 2009;9:162–174.
- Fontenot JD, Gavin MA, Rudensky AY. Foxp3 programs the development and function of CD4+CD25+ regulatory T cells. *Nat Immunol* 2003;4:330–336.
- Smyth MJ, Teng MW, Swann J, Kyriakopoulos K, Godfrey DI, Hayakawa Y. CD4+CD25+ T regulatory cells suppress NK cell-mediated immunotherapy of cancer. *J Immunol* 2006;176:1582–1587.
- Yu P, Lee Y, Liu W, et al. Intratumor depletion of CD4+ cells unmasks tumor immunogenicity leading to the rejection of late-stage tumors. *J Exp Med* 2005;201:779–791.
- Xu D, Gu P, Pan PY, Li Q, Sato AI, Chen SH. NK and CD8+ T cell-mediated eradication of poorly immunogenic B16-F10 melanoma by the combined action of IL-12 gene therapy and 4-1BB costimulation. *Int J Cancer* 2004;109:499–506.
- Crowe NY, Coquet JM, Berzins SP, et al. Differential antitumor immunity mediated by NKT cell subsets in vivo. *J Exp Med* 2005;202:1279–1288.
- Ghiringhelli F, Menard C, Terme M, et al. CD4+CD25+ regulatory T cells inhibit natural killer cell functions in a transforming growth factor- β -dependent manner. *J Exp Med* 2005;202:1075–1085.
- Ghiringhelli F, Menard C, Martin F, Zitvogel L. The role of regulatory T cells in the control of natural killer cells: relevance during tumor progression. *Immunol Rev* 2006;214:229–238.
- Raskovalova T, Huang X, Sitkovsky M, Zacharia LC, Jackson EK, Gorelik E. Gs protein-coupled adenosine receptor signaling and lytic function of activated NK cells. *J Immunol* 2005;175:4383–4391.
- Lokshin A, Raskovalova T, Huang X, Zacharia LC, Jackson EK, Gorelik E. Adenosine-mediated inhibition of the cytotoxic activity and cytokine production by activated natural killer cells. *Cancer Res* 2006;66:7758–7765.
- Rhule JT, Hill CL, Judd DA, Schinazi RF. Polyoxometalates in medicine. *Chem Rev* 1998;98:327–358.
- Hasenknopf B. Polyoxometalates: introduction to a class of inorganic compounds and their biomedical applications. *Front Biosci* 2005;10:275–287.
- Wolf AM, Wolf D, Steurer M, Gastl G, Gunsilius E, Grubeck-Loebenstien B. Increase of regulatory T cells in the peripheral blood of cancer patients. *Clin Cancer Res* 2003;9:606–612.
- Ratainirina N, Poli A, Michel T, et al. Control of NK cell functions by CD4+CD25+ regulatory T cells. *J Leukoc Biol* 2007;81:144–153.
- Priebe T, Platsoucas CD, Nelson JA. Adenosine receptors and modulation of natural killer cell activity by purine nucleosides. *Cancer Res* 1990;50:4328–4331.

35. Priebe T, Platsoucas CD, Seki H, Fox FE, Nelson JA. Purine nucleoside modulation of functions of human lymphocytes. *Cell Immunol* 1990;129:321–328.
36. Ryzhov S, Novitskiy SV, Zaynagetdinov R, et al. Host A(2B) adenosine receptors promote carcinoma growth. *Neoplasia* 2008;10:987–995.
37. Hasko G, Kuhel DG, Chen JF, et al. Adenosine inhibits IL-12 and TNF- α production via adenosine A2a receptor-dependent and independent mechanisms. *FASEB J* 2000;14:2065–2074.
38. Christensen LD, Andersen V. Natural killer cells lack ecto-5'-nucleotidase. *Nat Immun* 1992;11:1–6.
39. Miller JS, Cervenka T, Lund J, Okazaki IJ, Moss J. Purine metabolites suppress proliferation of human NK cells through a lineage-specific purine receptor. *J Immunol* 1999;162:7376–7382.
40. Raskovalova T, Lokshin A, Huang X, Jackson EK, Gorelik E. Adenosine-mediated inhibition of cytotoxic activity and cytokine production by IL-2/NKp46-activated NK cells: involvement of protein kinase A isozyme I (PKA I). *Immunol Res* 2006;36:91–99.
41. Hoskin DW, Mader JS, Furlong SJ, Conrad DM, Blay J. Inhibition of T cell and natural killer cell function by adenosine and its contribution to immune evasion by tumor cells. *Int J Oncol* 2008;32:527–535.
42. Leen AM, Rooney CM, Foster AE. Improving T cell therapy for cancer. *Annu Rev Immunol* 2007;25:243–265.
43. Beldi G, Enjyoji K, Wu Y, et al. The role of purinergic signaling in the liver and in transplantation: effects of extracellular nucleotides on hepatic graft vascular injury, rejection and metabolism. *Front Biosci* 2008;13:2588–2603.
44. Mizumoto N, Kumamoto T, Robson SC, et al. CD39 is the dominant Langerhans cell-associated ecto-NTPDase: modulatory roles in inflammation and immune responsiveness. *Nat Med* 2002;8:358–365.
45. Zhou Q, Yan J, Putheti P, et al. Isolated CD39 expression on CD4+ T cells denotes both regulatory and memory populations. *Am J Transplant* 2009;9:2303–2311.
46. Banz Y, Beldi G, Wu Y, Atkinson B, Usheva A, Robson SC. CD39 is incorporated into plasma microparticles where it maintains functional properties and impacts endothelial activation. *Br J Haematol* 2008;142:627–637.
47. Corriden R, Chen Y, Inoue Y, et al. Ecto-nucleoside triphosphate diphosphohydrolase 1 (E-NTPDase1/CD39) regulates neutrophil chemotaxis by hydrolyzing released ATP to adenosine. *J Biol Chem* 2008;283:28480–28486.
48. Lakshmikanth T, Burke S, Ali TH, et al. NCRs and DNAM-1 mediate NK cell recognition and lysis of human and mouse melanoma cell lines in vitro and in vivo. *J Clin Invest* 2009;119:1251–1263.
49. Degli-Esposti MA, Smyth MJ. Close encounters of different kinds: dendritic cells and NK cells take centre stage. *Nat Rev Immunol* 2005;5:112–124.
50. Martin-Fontecha A, Thomsen LL, Brett S, et al. Induced recruitment of NK cells to lymph nodes provides IFN- γ for T(H)1 priming. *Nat Immunol* 2004;5:1260–1265.
51. Assarsson E, Kambayashi T, Schatzle JD, et al. NK cells stimulate proliferation of T and NK cells through 2B4/CD48 interactions. *J Immunol* 2004;173:174–180.
52. Hilchey SP, Kobie JJ, Cochran MR, et al. Human follicular lymphoma CD39+ infiltrating T cells contribute to adenosine-mediated T cell hyporesponsiveness. *J Immunol* 2009;183:6157–6166.
53. Mandapathil M, Szczepanski MJ, Szajnik M, et al. Increased ectonucleotidase expression and activity in regulatory T cells of patients with head and neck cancer. *Clin Cancer Res* 2009;15:6348–6357.
54. Mandapathil M, Hilldorfer B, Szczepanski MJ, et al. Generation and accumulation of immunosuppressive adenosine by human CD4+CD25^{high}FOXP3+ regulatory T cells. *J Biol Chem* 2010;285:7176–7186.
55. Stagg J, Divisekera U, McLaughlin N, et al. Anti-CD73 antibody therapy inhibits breast tumor growth and metastasis. *Proc Natl Acad Sci U S A* 107:1547–1552.

Received November 10, 2009. Accepted May 13, 2010.

Reprint requests

Address requests for reprints to: Simon C. Robson, MD, PhD, 330 Brookline Avenue, E/CLS-612, Beth Israel Deaconess Medical Center, Boston, Massachusetts 02215. e-mail: srobson@bidmc.harvard.edu; fax: (617) 735-2930.

Acknowledgments

The authors thank members of the Longwood Small Animal Imaging Facility of BIDMC for assistance with the in vivo bioluminescence imaging.

X.S. and Y.W. contributed equally to this work, and the surnames are arranged alphabetically.

Conflicts of interest

The authors disclose no conflicts.

Funding

This study has been supported by the National Institutes of Health (NHLBI P01-HL076540 and R01-HL094400).

Luminescence Imaging of Regenerating Free Bone Graft in Rats

Asako Yamaguchi, M.D.
Takashi Murakami, M.D.,
Ph.D.
Masafumi Takahashi, M.D.,
Ph.D.
Eiji Kobayashi, M.D., Ph.D.
Yasushi Sugawara, M.D.,
Ph.D.

Shimotsuke, Tochigi, Japan

Background: Bone transplantation is an important procedure often used for bone defect reconstruction after trauma and malignancies. However, the kinetics of free bone graft-derived cells remains unclarified. The authors examined the kinetics of graft-derived cells using transgenic rats systemically expressing firefly luciferase.

Methods: Free iliac bone grafts ($5 \times 5 \times 2$ mm, $n = 10$) derived from luciferase transgenic rats were transplanted into the subcutaneous space of the back of wild-type Lewis rats, and the kinetics of graft-derived cells were evaluated over time by determining the level of luminescence emission.

Results: Although the luminescence level emitted by luciferase decreased after transplantation, a substantial luminescence level (mean, 1.6×10^7 photons/second) was emitted from donor-derived cells even at 180 days after transplantation, suggesting a long-term survival of graft-derived cells. In a computed tomographic image analysis of bone grafts retrieved 180 days after transplantation, high-luminescence grafts with a sufficient number of viable graft-derived cells (mean, 2.6×10^7 photons/second; $n = 4$) showed significantly higher bone graft volume (3.1-fold) and polar moment of inertia of area (7.2-fold) than low-luminescence grafts (mean, 1.0×10^7 photons/second; $n = 4$), indicating that high-luminescence grafts maintain better conditions.

Conclusion: These results suggest that bone graft-derived cells can survive for a long time and that the presence of a sufficient number of viable graft-derived cells is essential for graft engraftment and remodeling. (*Plast. Reconstr. Surg.* 127: 78, 2011.)

Bone transplantation is a basic surgical procedure used for reconstruction of bone defects from cancer or trauma and treatment of congenital anomalies of the extremity, such as brachydactyly. However, the procedure may not lead to substantial healing because of infection or resorption of the bone graft.

Various studies have been conducted on free bone transplantation. One of the concepts that has been supported for a long time is that of "creeping substitution," in that a large part of the cellular component of a free bone graft dies within a few days, followed by gradual absorption and replacement starting at the part in contact with a viable graft.¹ Although some studies have shown

that cells in bone grafts eventually die,² others have demonstrated that cells located approximately $300 \mu\text{m}$ from the cortical bone surface of the bone graft survive.^{3,4} Recent studies have also shown the survival of bone graft-derived cells.⁵ It is clinically and experimentally known that fresh autologous bone grafts can achieve better engraftment than allogeneic or preserved bone grafts.⁶ However, little is known regarding whether graft-derived cells can survive or not.

Luciferase-transgenic rats, in which the luciferase gene is transfected so that cells in almost all parts of the body have luciferase activity, have recently been developed.⁷ The use of these genetically engineered animals has enabled us to examine the time course of the viability of transplanted cells in live animals using luciferase luminescence

From the Division of Plastic Surgery, Department of Surgery, the Division of Bioimaging Sciences Center for Molecular Medicine, and the Center For Development of Advanced Medical Technology, Jichi Medical University.

Received for publication February 18, 2010; accepted June 22, 2010.

Copyright ©2010 by the American Society of Plastic Surgeons

DOI: 10.1097/PRS.0b013e3181f959b2

Disclosure: *The authors have no commercial, proprietary, or financial interests related to the information in this article.*

as a marker. Specifically, administration of the luminescence substrate luciferin to these animals results in the emission of luminescence intensity that is dependent on the amount of adenosine triphosphate produced in cells, enabling us to visually and quantitatively evaluate cell viability by measuring luminescence level.

In this study, we demonstrated that graft-derived cells are capable of long-term survival and determined the role of these cells in graft acceptance. These experimental results may have an implication to the long-term survival of free bone grafts, which are commonly applied in clinical practice.

MATERIALS AND METHODS

Experimental Design

All surgical interventions and animal care were performed in accordance with Jichi Medical University Guide for Laboratory Animals. Lewis rats were purchased from Charles River Japan (Yokohama, Japan). All surgical procedures were performed under anesthesia with intraperitoneal injection of Nembutal (Abbott, Chicago, Ill.). All rats were housed in cages and allowed normal cage activity without any restrictions. All animals were euthanized by means of an anesthetic overdose injection at final evaluation. All experiments were carried out using 10-week-old male rats.

Surgical Procedure: Free Bone Transplantation and Vascularized Bone Transplantation

A vascularized tibial transplant model of the Lewis rat was established.⁸ A 2.5-cm tibiofibular complex with cartilage removed from the knee joint surface on the tibial side and with a vascular pedicle of the femoral artery and vein was used as a vascularized bone graft. The vessels were anastomosed to the femoral artery and vein of a recipient rat with a 10-0 nylon suture under a microscope. The ischemic time during this procedure was approximately 30 minutes. The vascularized bone graft was implanted into a subcutaneous pocket formed in the right inguinal region, and another tibiofibular complex without a vascular pedicle collected from the other leg of the same donor rat was implanted as a free bone graft in the left inguinal region ($n = 3$). The wound was opened 14 days postoperatively, and the patency test of the anastomosed vessels was performed under a microscope. At the same time, the bone grafts were removed for histologic examination.

In Vivo Bioluminescence Imaging

Luciferase-expressing Lewis transgenic rats were used.⁷ To visualize luciferase expression *ex vivo* and *in vivo*, an *in vivo* bioimaging system (IVIS; Xenogen, Alameda, Calif.) was used. To detect photons from luciferase-expressing cells, D-luciferin (potassium salt; Biosynth, Postfach, Switzerland) was injected into the penile vein of anesthetized rats (30 mg/kg body weight) with isoflurane (Abbott). Lucimages were taken using IVIS and quantified using the IVIS Living Image software (Xenogen) package. Data were expressed as photons per second per square centimeter per steradian.

To examine whether the living bone derived from luciferase-expressing Lewis transgenic rats emitted luminescent light, fresh bones and bones demineralized by freezing twice for 5 minutes in liquid nitrogen were tested ($n = 3$). Macroscopic images were acquired in a drop of phosphate-buffered saline. Next, iliac free bone grafts ($5 \times 5 \times 2$ mm) from luciferase-expressing Lewis transgenic rats were transplanted into the subcutaneous space of recipient wild-type Lewis rats ($n = 10$). As a control, iliac bone grafts ($5 \times 5 \times 2$ mm) were also collected from wild-type Lewis rats and transplanted into the subcutaneous pockets of recipient rats using the same procedure ($n = 4$). Post-transplantation measurement consisted of 10 sequential sessions of 1-minute measurement, so that luminescence intensity could be recorded over time.

Detection of LacZ Expression by Immunohistochemistry

LacZ-transgenic rats is derived from LEW (Rosa/LacZ-Lew) rats driven under the ROSA 26 promoter.⁸ Free iliac bone transplantation ($5 \times 5 \times 2$ mm) from LacZ-transgenic rats to wild-type Lewis rats was performed ($n = 4$). Transplanted bone grafts were removed at various time points after transplantation for immunohistochemistry.

An iliac bone collected from a LacZ-transgenic rat was used as positive control, and an iliac bone collected from a wild-type Lewis rat was used as a negative control ($n = 4$). Bone tissues were fixed in 10% formalin at ambient temperature for 2 days, followed by decalcification in 10% ethylenediaminetetraacetic acid solution at ambient temperature for 14 days. Tissues were then paraffin-embedded and sliced into 5- μ m sections.

LacZ expression was evaluated by immunohistochemistry using anti- β -galactosidase rabbit polyclonal antibody (1:1500; Biogenesis, Poole,